

PARASOL: Parametric Style Control for Diffusion Image Synthesis

Gemma Canet Tarrés¹, Dan Ruta¹, Tu Bui¹, John Collomosse^{1,2}

¹University of Surrey, ²Adobe Research

{g.canettarres, d.ruta, t.v.bui, j.collomosse}@surrey.ac.uk

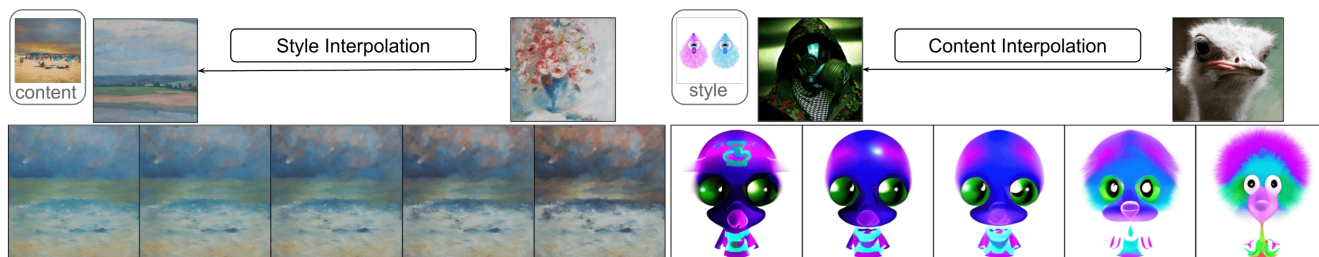


Figure 1. Images generated using PARASOL. Leveraging parametric style control and multi-modal synthesis, we demonstrate the ability of our model to synthesize creative images by interpolating different styles (left) or contents (right).

Abstract

We propose *PARASOL*, a multi-modal synthesis model that enables disentangled, parametric control of the visual style of the image by jointly conditioning synthesis on both content and a fine-grained visual style embedding. We train a latent diffusion model (LDM) using specific losses for each modality and adapt the classifier-free guidance for encouraging disentangled control over independent content and style modalities at inference time. We leverage auxiliary semantic and style-based search to create training triplets for supervision of the LDM, ensuring complementarity of content and style cues. *PARASOL* shows promise for enabling nuanced control over visual style in diffusion models for image creation and stylization, as well as generative search where text-based search results may be adapted to more closely match user intent by interpolating both content and style descriptors.

1. Introduction

Deep generative models have immense potential for creative expression, yet their controllability remains limited. In particular, diffusion models can synthesize high-quality and diverse outputs, yet their ability for *fine-grained control* of attributes such as visual style is often constrained by reliance on discrete text-based prompts or image exemplars. By contrast, visual search models often use parametric style embeddings to achieve this more nuanced control. We propose Parametric Style Control (PARASOL) to bridge this gap. PARASOL is a novel synthesis model that enables disentangled control over the visual style of an im-

age, conditioning synthesis on both a semantic cue and a fine-grained visual style embedding (ALADIN [37]). We demonstrate the potential of this framework for generative search by adapting text-based search results to match user intent and by interpolating one or both of content and style descriptors. Our technical contributions are:

Fine-grained style-conditioned diffusion. We synthesize images using a latent diffusion model (LDM) conditioned on multi-modal input describing independent content and style descriptors, trained using a joint loss that encourages disentangled control. At inference time we invert the content image back to its noised latent, and re-run the denoising process incorporating our content and style conditioning together with modality-specific classifier-free guidance, enabling fine-grained control over the target and influence of each modality.

Cross-modal training via search. We use auxiliary semantic and style based search models to form triplets (content input, style input, image output) for supervision of the LDM training, ensuring complementarity of the content and style cues to encourage disentangled control at inference. ¹

PARASOL leverages the ALADIN parametric embedding [37] (proposed originally for searching stylized artwork) for fine-grained style control. Yet PARASOL can also be applied for search itself. We briefly show that coupling PARASOL with text encoders for ALADIN embedding also enables application to *generative search* enabling fine-grained adaptation of results from text-based search queries to enable users to iterate on search results to more closely match their search intent.

¹We release these training data as an additional contribution.

2. Related Work

Style transfer and representation. Neural style transfer (NST) has classically relied upon aligning statistical features [18, 27] extracted from pretrained models (e.g. VGG [11]) in the output image with those of an exemplar style image. More recently, style feature representations are learned via self-attention (AvatarNet [40], SANet [30]). PAMA [28] further improve upon this through progressive multi-stage alignment of features, improving consistency of style across the stylized image. ContraAST [5] introduce contrastive losses and domain-level adversarial losses to improve similarity of stylized images to real style images. CAST [53] refine this by including ground truth style images into the contrastive objective. Style transfer methods always aims to alter texture while retaining exact content of an image, hindering creativity and controllability in image generation. In this work, we aim at bridging this gap.

Cross-modal and style search. Early cross-modal retrieval work focused on canonical correlation analysis [12, 23]. Deep metric learning approaches typically explore dual encoders unified via recurrent or convolutional layers combined with metric learning over the joint embedding, using triplet or contrastive losses. Recently transformer encoders are popular in such frameworks, including BERT [21] and derivatives for language and ViT [8] based image representations. Vision-language models such as CLIP [31] have been shown effective for search and conditional synthesis.

For style, earlier style transfer work [9] explore representation learning of artistic style in the context of fine art, learning 10 styles to generalize a style transfer model to more than a single style. Also leveraging a labelled triplet loss [6] learn a metric style representation over a subset of the BAM dataset [45], but are limited by the available style labels in BAM, covering only 7 styles. ALADIN [37] first explored a fine-grained style representation learning through multi-layer AdaIN [18] feature extraction, trained over their newly introduced BAM-FG dataset. This was evolved in StyleBabel [36] by replacing the architecture with a vision transformer [8], which we use in our work.

Multi-modal conditional image generation. Due to the outstanding quality of recent image generation methods, conditional image generation is currently becoming a focus of attention in research. These aim to achieve a more controllable synthesis. Most conditional methods consider a single input modality (e.g. text [38, 29, 34, 33, 13], bounding box layouts [44, 54, 43], scene graphs [20, 1]) and a few accept multi-modal conditions. VAEs [22] have often been used for this task, since they allow learning a joint distribution over several modalities while enabling joint inference given a subset [47, 42, 24].

GAN-based methods follow different conditioning strategies. TediGAN [48] relies on a pretrained unconditional generator, IC-GAN [4] is based on a conditional GAN that leverages search for synthesizing new images. PoE-

GAN [19] uses a product of experts GAN to combine several modalities (sketch, semantic map, text) into an image.

Make-A-Scene [10] and CoGS [15] leverage the benefits of transformers and learned codebooks for incorporating multimodal conditioning. They both encode each modality independently into discretized embeddings that are modelled jointly by the transformer.

More recently, several multi-modal diffusion-based image generation methods have been proposed. DiffuseIT[25] and CDCD [55] combine the different modalities by tuning specific losses. Others make use of multimodal embeddings, such as CLIP [31] for combining text and image-based inputs [17] or even retrieve auxiliary similar images to further condition the network [3, 41, 35]. eDiffi [2] uses specific single-modality encoders and incorporates all embeddings through cross-attention at multiple resolutions. ControlNet [51] and MCM [14] explore the integration of new input modalities as extra conditioning signals by leveraging the frozen Stable Diffusion model [34]. In contrast, we train our latent diffusion with explicit governing loss for each input modality (i.e. content and style).

3. Methodology

We propose PARASOL; a method to creatively synthesize new images from fine-grained style and content information. We design PARASOL to maximize fine-grained control over the structure and style. The main design choices that lead to that are as follows:

- By incorporating a parametric style encoder (ALADIN [37]) in our pipeline, more nuanced disentangled style information is provided to the network, allowing the fine-grained style to be transferred.
- The metric properties of both modality-specific encoders allow multiple styles and/or semantics to be combined and interpolated for generating highly-creative content.
- An inverse diffusion step is incorporated at sampling time for allowing content details and structure to be preserved throughout the image generation process.
- A specific classifier-free guidance format is introduced for enabling each modality to independently influence the image generation.

The core of PARASOL is a pre-trained LDM [34] fine-tuned for accommodating multimodal conditions. The pipeline (Fig. 2) consists of six components: 1) An Autoencoder for encoding/decoding images into the diffusion latent space; 2) A U-Net based denoising network; 3) A fine-grained style encoder enabling parametric control over visual appearance; 4) A semantic encoder to express content control; 5) A projector network to bridge both modalities into the same feature space for model conditioning; 6) An optional post-processing step for colour correction.

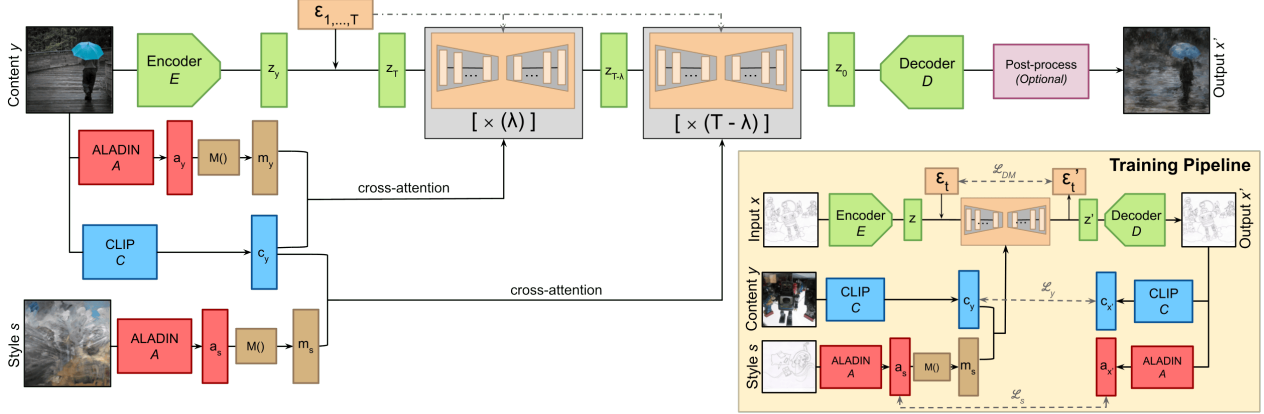


Figure 2: Illustration of the full PARASOL pipeline. It consists of six components: A parametric style encoder (red); A projector network (brown); A semantics encoder (blue); An Autoencoder (green); A denoising U-Net (orange); An optional post-processing step (purple). At training time (bottom-right corner), two modality-specific losses (L_s and L_y) are used to encourage disentanglement. They are combined with L_{DM} and minimized in the training. At inference time (big pipeline), a parameter $\lambda \in [0, T]$ is introduced. After λ denoising steps, the style condition is changed for transferring a new style.

3.1. Obtaining Training Supervision Data via Cross-Modal Search

A dataset of triplets (x, y, s) is required to fine-tune the LDM that PARASOL is based on. In each set, the output image x is a stylistic image matching the artistic style of the style image s , and semantic content of the content image y .

This dataset is built via cross-modal search for the two input modalities: content and style. Given an image x , its semantics descriptor $c_x = C(x)$ and style descriptor $a_x = A(x)$ are computed using parametric modality specific encoders (C and A). Leveraging their parametric properties, the most similar images for each modality can be retrieved by finding the nearest neighbours in the respective feature spaces.

Some restrictions are applied to ensure disentanglement between both input modalities. First, different data is indexed for each modality’s search. A set of images with stylistic and aesthetic properties is defined as the ”Style Database” (\mathcal{S}). These are indexed using a parametric style encoder and used to find the style image s . In parallel, a set of photorealistic images with varied content is defined as the ”Semantics Database” (\mathcal{C}) and is indexed using a parametric semantics encoder for finding the content image y .

Using a_x as query, the top k most style similar images in \mathcal{S} are retrieved as candidates for the style image s . Their similarity to x in the semantics feature space is computed and they are discarded as candidates if this similarity is over a certain threshold. Finally, the style image s is picked as the closest image in \mathcal{S} fulfilling all restrictions. Using the semantics description c_y as query, same procedure is conducted for finding the content image y in \mathcal{C} (See SupMat.).

3.2. Encoding the Style and Semantics Inputs

Given a triplet (content image y , style image s , output image x), the diffusion model is trained to reconstruct x by

conditioning on y and s , after encoding the style and content images through the respective encoders.

Arguably, the same pre-trained encoder could be used to describe both modalities (*e.g.* RDM [3]). However, the use of modality-specific encoders pre-trained on task-specific curated data has been beneficial for conditioning the diffusion process [38]. Furthermore, using a condition-specific encoder (*i.e.* style or semantics specific) strongly contributes to disentangling the content and style features and enables separate and independent conditioning of the network on each attribute.

Nonetheless, using a different encoder for each modality poses a new challenge. In most cases, their representations won’t have the same format or belong to the same feature space. Fine-tuning an LDM that was pre-trained on one conditional modality to understand and incorporate the information of two separate modalities can be very data and compute demanding. Therefore, we train an MLP-based projector network $M()$ to obtain a joint space for both descriptors. The network takes the style descriptor a_s of s as input and projects it into a new embedding m_s that lies in the same feature space as c_y , the semantics descriptor of y .

3.3. Incorporating Latent Diffusion Models

PARASOL is built on top of a pre-trained LDM. This pre-trained model has two components: An Autoencoder and a U-Net denoising network. The Autoencoder is kept frozen throughout our training, while the U-Net is fine-tuned to accommodate the new conditions. The first component consists of an Encoder \mathcal{E} and a Decoder \mathcal{D} . For each image x , the encoder \mathcal{E} embeds it into $z = \mathcal{E}(x)$, while the decoder \mathcal{E} can reconstruct $x' = \mathcal{D}(z)$ from z . The diffusion takes place in the Autoencoder’s latent space.

3.3.1 Latent Diffusion Model Background

Let $q(\cdot)$ be a data distribution and z a sample from it. Small amounts of Gaussian noise $\epsilon_t, t = 1, \dots, T$ can be sequentially added to the variable z to create a Markov chain of noisy variables z_t . The diffusion model learns $q(\cdot)$ by denoising z_t through a reverse process of the Markov Chain, referred to as the "Reverse Diffusion Process".

Since this process is not directly computable, we use neural networks to approximate this. Thus, diffusion models can be interpreted as a sequence of denoising autoencoders $\epsilon_\theta(z_t, t)$ that estimate z_{t-1} from its noisier version z_t . Through a reparametrization trick [16, 34], each of these denoising autoencoders can be trained to minimize:

$$L_{DM} = \mathbb{E}_{z_t, \epsilon_t \sim \mathcal{N}(0,1), t} [\|\epsilon_t - \epsilon'_t\|^2], \quad (1)$$

where $\epsilon'_t := \epsilon_\theta(z_t, t)$.

3.3.2 Conditioning through Cross-Attention

In our training, we fine-tune the LDM to incorporate multi-modal conditions. In particular, the diffusion process needs to be conditioned on two independent signals: m_s and c_y . We adapt the denoising autoencoder ϵ_θ to condition on both signals as well as on the noisy sample z_t and the timestamp t : $\epsilon_\theta(z_t, t, m_s, c_y)$. Inspired by [34, 3], we incorporate these new signals into the U-Net backbone through the use of cross-attention by stacking the two signals m_s and c_y together and mapping them into every intermediate layer of the U-Net via cross-attention layers. As a result, at each timestep t , the output z_{t-1} of the model ϵ_θ is computed taking both conditions m_s and c_y into account.

3.3.3 Conditioning using Classifier-free Guidance

As presented in [29, 7], samples from conditional diffusion models can be improved by the use of a classifier(-free) guidance. The idea behind this is to additively perturb the mean and variance of the diffusion model by the gradient of the log-probability of the conditioning modality leading to the generation of a particular image.

We extend the idea of classifier-free guidance for independently accommodating multiple modalities. In training time, both input conditions are replaced by a null condition $\epsilon_\theta(z_t, t, \emptyset, \emptyset)$ with a fixed probability so that the network can learn how to produce unconditional outputs. Then, at sampling time, this output is guided towards $\epsilon_\theta(z_t, t, m_s, \emptyset)$ and $\epsilon_\theta(z_t, t, \emptyset, c_y)$ and away from $\epsilon_\theta(z_t, t, \emptyset, \emptyset)$ as:

$$\begin{aligned} \epsilon_\theta(z_t, t, m_s, c_y) &= \epsilon_\theta(z_t, t, \emptyset, \emptyset) \\ &+ g_s [\epsilon_\theta(z_t, t, m_s, \emptyset) - \epsilon_\theta(z_t, t, \emptyset, \emptyset)] \\ &+ g_y [\epsilon_\theta(z_t, t, \emptyset, c_y) - \epsilon_\theta(z_t, t, \emptyset, \emptyset)] \end{aligned} \quad (2)$$

The parameters g_s and g_y are therefore introduced to determine how much weight the style or semantics inputs have in the image generation process. Thus, by tuning the ratio of the two parameters g_s and g_y , the user can approximate the degree of influence the style and semantics inputs have

over the output. However, it is important to note high values of either parameter will lead to higher quality images and lower diversity in the outputs.

3.4. Training Pipeline

PARASOL is trained by finetuning the pre-trained model in [3]. At each training step, a random timestep $t \in [1, T]$ is selected. In Fig 2, each training image x is encoded into z using the pre-trained encoder \mathcal{E} and noised with Gaussian noise ϵ_t . Similar images in terms of style s and content y are encoded into m_s and c_y . The embedding z_t is then fed into the U-Net denoising autoencoder, which is also conditioned on m_s and c_y through cross-attention. This network, along with the projector network $M(\cdot)$ are the only parts of the pipeline that are being trained.

3.4.1 Training Objectives

Training is done by minimizing a combination of 3 losses:

Diffusion Loss (Eq. (1)) minimizes the distance between the predicted noise ϵ'_t and the true noise ϵ_t , in estimating z_t .

Modality-Specific Losses For encouraging the output image to have the same style as s and the same semantics as y , the style and semantics of the reconstructed image x' are encoded through the use of a style and a semantics encoder, respectively. The two losses are thus computed as: $L_s = \text{MSE}(a_s, a_{x'})$ and $L_y = \text{MSE}(c_y, c_{x'})$.

Total Loss All three losses are combined in a weighted sum and simultaneously optimized:

$$L = L_{DM} + \omega_s \cdot L_s + \omega_y \cdot L_y \quad (3)$$

3.5. Sampling Pipeline

When sampling (Fig. 2), an inversion process takes place to ensure the fine-grained content details in y are preserved in the final image. First, the semantics image y is encoded via \mathcal{E} and noised through a complete forward diffusion process. During this process, the noise ϵ_t introduced at each timestep $t = 1, \dots, T$ is being saved. Next, the Reverse Diffusion Process described in Section 3.3.1 takes place by denoising with the saved ϵ_t values at each step. If the input conditions are not changed throughout the whole denoising process, the image y is faithfully reconstructed. For offering the possibility of transferring a new style while preserving the fine-grained content details in the image, a parameter $\lambda \in [1, T]$ is introduced. In the first λ denoising steps, the U-Net is conditioned through cross-attention on the style and semantics descriptors of y , while in the last $T - \lambda$ steps, the style condition is switched to m_s , the encoded style from s .

Therefore, setting λ close to T leads to more structurally similar images to y while lower λ values generate images more stylistically similar to s .

3.5.1 Colour Distribution Post-Processing

A challenge with perceptually matching the style of a reference image s through diffusion, is mis-matched colour dis-

tribution, despite image fidelity to y . We offer the possibility of addressing this issue via additional post-processing steps inspired by ARF [50]. In this optional step, the generated image is modified to match the mean and covariance of the style image, shifting the colour distribution.

4. Results and Discussion

We discuss our experimental setup and evaluation metrics in Section 4.1 and compare to baselines (Section 4.2) and different ablations (Section 4.3). We showcase user control of PARASOL in experiments in Section 4.4, and its use as a generative search model for improving fine-grained control is investigated in Section 4.5.

4.1. Experimental Setup

Network and training parameters. We use a pre-trained ALADIN [37] as parametric style encoder and the pre-trained "ViT-L/14" CLIP [31] model for encoding the content input. The Autoencoder and U-Net are used from [3]. The U-Net is fine-tuned using a multimodal loss (Eq. (3)) with weights $\omega_s = 10^5$ and $\omega_y = 10^2$.

At sampling time, unless stated otherwise, we use $\lambda = 20$, $g_s = 5.0$ and $g_y = 5.0$ and no post-processing in our experiments and figures.

Dataset. The final model and all the ablations are trained using our own set of 500k triplets obtained as described in Section 3.1. Images x are obtained from BAM-FG [37], while style images s are extracted from BAM (Behance Artistic Media Dataset) [46] and content images y are parsed from *Flickr*. BAM-FG is a dataset that contains 2.62M images grouped into 310K style-consistent groupings. Only a subset of stylized non-photorealistic images from BAM-FG with a semantically rich content are considered for building our training triplets.

For the Generative Search experiment, a subset of 1M images from BAM is indexed and used for search, while ensuring no intersection with the images used for training.

Evaluation metrics. We measure several properties of the style transfer quality in our experiments. LPIPS [52] is a perceptual metric for measuring semantic similarity between the content and stylized image, SIFID [39] to measure style distribution similarity, and Chamfer distance to measure colour similarity. We use Chamfer distance normalized by the number of pixels in the image, to maintain comparable values for any image resolution. Additionally, we compute the MSE based on ALADIN embeddings to measure style similarity between the synthesized image and the input style and MSE based on CLIP embeddings for quantifying its semantic similarity to the content input.

4.2. Comparison to Baselines

We compare to several generative multimodal diffusion-based models as well as NST models. For the latter, most diffusion-based models are text-based, so we resource to state of the art non-diffusion based models.

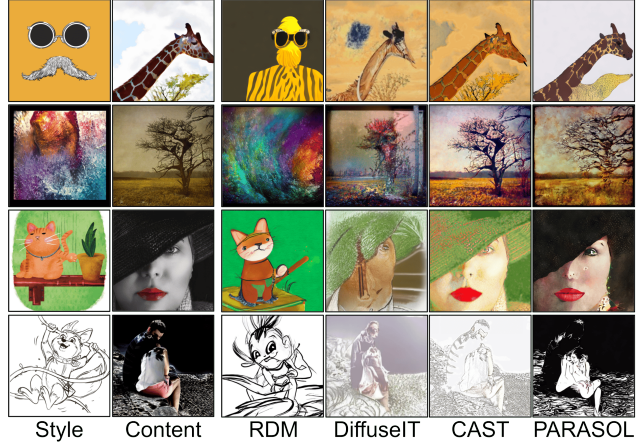


Figure 3: Representative examples from RDM [3], DiffuseIT [25], CAST [53] and PARASOL. For simplicity, only the baselines with the best performance in the user study (Table 2) are visualized in this figure.

Method	SIFID↓	LPIPS↓	ALADIN-MSE↓	CLIP-MSE↓	Chamfer↓
RDM	3.937	0.736	3.945	12.792	1.431
ControlNet	4.265	0.757	5.148	16.944	3.612
DiffuseIT	2.572	0.677	4.460	15.159	0.184
CAST	6.106	0.608	4.633	16.732	0.188
ContrAST	2.791	0.651	4.171	16.111	0.126
PAMA	2.509	0.659	4.411	16.194	0.287
SANet	2.608	0.671	4.200	16.187	0.301
PARASOL	2.994	0.525	4.054	15.12	1.847
PARASOL+	2.293	0.679	3.891	14.999	0.340

Table 1: Quantitative comparison of style (SIFID, ALADIN-MSE, Chamfer) and content (LPIPS, CLIP-MSE) metrics. We include our optional post-processing as PARASOL+. Chamfer scores are scaled down $\times 10^{-3}$.

RDM [3] share its backbone with PARASOL, the main difference being using CLIP for encoding all conditions. For fair comparison, we fine tune it on our training triplets.

DiffuseIT [25] propose a diffusion-based image translation method guided by a semantic cue. Several losses ensure consistency in style and structure. Since no training code is provided, we resource to the ImageNet pre-trained model.

ControlNet [51] propose the training of a neural network for incorporating task-specific conditions into the generation process. Since it only accepts textual prompts as input, we extract captions from our content images using BLIP [26] and train the network to be conditioned by style images via our training triplets.

Style transfer We evaluate our method against four recent NST models: CAST [53], PAMA [28], SANet [30], and ContraAST [5]. Each of these methods is prompt-free, and are thus directly comparable to our method.

Quantitative evaluations using the metrics described in Section 4.1 are provided in Table 1.

Our complete method produces the best SIFID and

Method	Pref. Overall	Pref. Style Fidelity	Pref. Content Fidelity
RDM	17.60%	18.40%	9.20%
ControlNet	1.20%	0.00%	1.60%
DiffuseIT	29.20%	34.80%	27.20%
PARASOL	52.00%	46.80%	62.00%
CAST	20.40%	11.20%	33.60%
ContrAST	15.20%	12.00%	10.40%
PAMA	17.60%	8.40%	8.40%
SANet	16.40%	9.60%	7.20%
PARASOL	30.40%	58.80%	40.40%

Table 2: Evaluation of our method vs. all different baselines based on AMT experiments. Due to limited screen space, we divide the baselines in two separate experiments: comparing to image generation methods, and to NST methods. In both cases, we ask workers to choose their preferred image in terms of: 1) image quality, 2) style fidelity and 3) content fidelity (via 3 separate experiments).

ALADIN-MSE scores proving to be a strong method for style transfer. The measure of semantics similarity to the content input through CLIP-MSE and LPIPS is comparable to the other methods. Although our Chamfer score is improvable, we highlight the ability of our method for tuning the influence of style and structure influence. If style and colour similarity are a priority for the user, the different parameters in the model can be adapted for providing more stylistically similar images to the style input.

The optional post-processing step drastically improves Chamfer distances, and SIFID metrics. However, the LPIPS scores are worse. While this is not unexpected, it highlights a weakness with LPIPS, as a metric in measuring content similarity. The re-colouring steps change only the colours in the image, not modifying any content.

We undertake a user study (Table 2) using Amazon Mechanical Turk (AMT), to support our quantitative metrics. In these, workers are shown a content image, a style image and a set of images generated using our method and different baselines. For fairness, we compare to the version of our method without the post-processing step. PARASOL was chosen as the preferred method in all categories, measured via majority consensus voting (3 out of 5 workers). Fig. 3 shows visual examples of the most competitive baselines.

4.3. Ablation Study

Considering the available pre-trained RDM model conditioned on CLIP embeddings as our baseline, we justify the addition of each component in our pipeline through an ablation study (Table 3).

Switching the style encoder from CLIP to ALADIN offers a lot of benefits in terms of disentanglement and fine-grained style information. However, even when fine-tuning the network on the new descriptors, it is not able to understand the nature of the new representations. Table 3 shows the substantial improvement of all metrics when the

Method	SIFID↓	LPIPS↓	ALADIN-MSE↓	CLIP-MSE↓	Chamfer↓
PARASOL -(I, L, M, Ft, A)	3.077	0.749	4.312	15.428	0.127
PARASOL -(I, L, M, Ft)	7.759	0.813	5.540	17.457	1.184
PARASOL -(I, L, M)	6.883	0.777	4.356	15.887	0.788
PARASOL -(I, L)	4.269	0.748	3.573	14.740	0.174
PARASOL -(I)	4.329	0.747	3.564	14.714	0.155
PARASOL	2.994	0.525	4.054	15.12	1.847
PARASOL+	2.293	0.679	3.891	14.999	0.340

Table 3: Quantitative evaluation metrics for different ablations of our final model. Considering pre-trained RDM as the baseline, this study justifies: 1) The use of a parametric style encoder (A); 2) The need to fine-tune the model (Ft); 3) The addition of a projector network for the style embedding (M); 4) The effect of modality-specific losses (L); 5) The design choice of inverting the diffusion process (I); 6) The use of the optional post-processing step (PARASOL+).

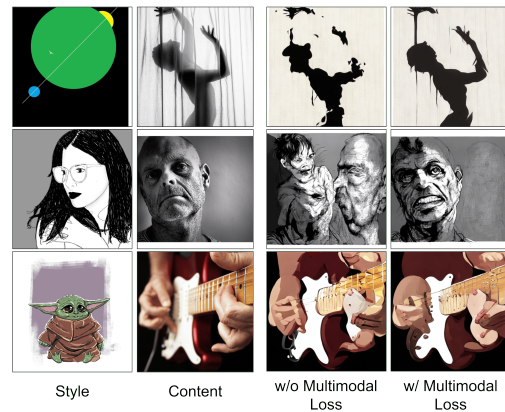


Figure 4: Visualization of synthetic images from different ablations of our method. The addition of the loss lessens the presence of artifacts generated from any remaining content information in the style descriptor and encourages a better semantic understanding of the content image.

projector $M()$ is introduced, proving its crucial role in the pipeline. As illustrated in Fig. 4, the multimodal loss assists the network in further disentangling both modalities.

Despite some lower metrics when using inversion, we consider it beneficial overall, due to the added controllability, and improved style transfer metrics (SIFID, LPIPS).

4.4. Controllability Experiments

We demonstrate four ways PARASOL can be used to exert control over the image synthesis process.

4.4.1 Disentangled Style and Content

We propose different ways of controlling the influence of each input modality in the image generation process.

Via inversion The parameter λ (Sec. 3.5) enables choosing at which step of the inversion process the style condition is changed (Fig. 5).

Via classifier-free guidance parameters The values g_s and g_y (Eq. (2)) determine how much weight each condition

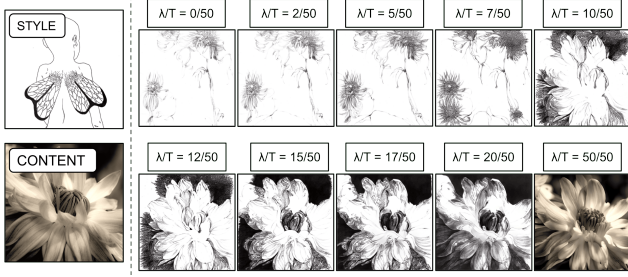


Figure 5: Effect of λ . Images synthesized from the same style and content information by using 10 different values of λ . Higher λ values ensure a more faithful structure to the input, while lower values further encourage style transfer.

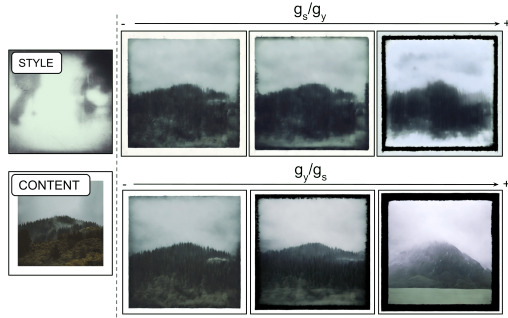


Figure 6: Effect of g_s and g_y . First row: the value of g_y is kept constant while g_s is increased, showing more influence from the input style information. Second row: g_s is constant and g_y is increased, obtaining a more notable semantic influence from the conditioning content cue.

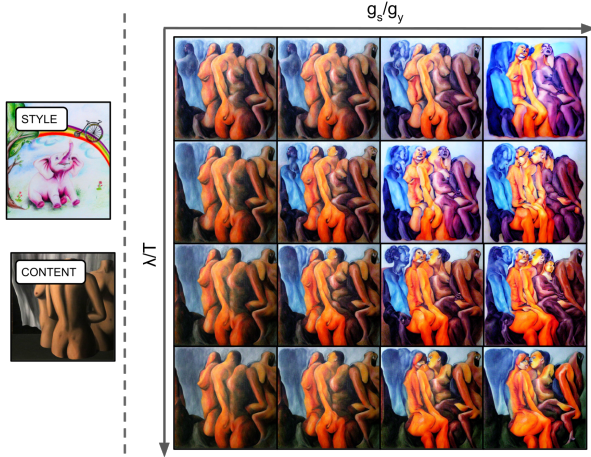


Figure 7: Effect of λ and g_s . Top rows (low λ) show more creative structures. Right columns (high g_s) offer highly stylized images. Bottom-left corner (high λ , low g_s) is the closest to the unstylized content input.

has in the image generation process. (Fig. 6).

Via both sets of parameters By fixing g_y and tuning g_s and λ , a trade-off between stylization and structure fidelity can be defined (Fig. 7).

User Study	RDM	DiffuseIT	PARASOL
Pref. Content Interpolation	12.037%	43.518%	44.444%
Pref. Style Interpolation	16.808%	31.932%	51.260%

Table 4: AMT user evaluation of content and style interpolations. Our method is compared to RDM [3] and DiffuseIT [25] in terms of sets of images generated via style and content interpolations. Model preference is measured via majority consensus voting (3 out of 5).

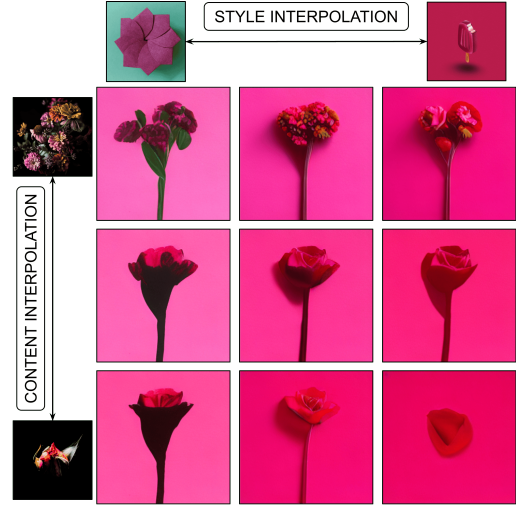


Figure 8: Style and content interpolation. Images generated by interpolating two styles and two content images.

4.4.2 Content and Style Interpolation

PARASOL can synthesize images by interpolating different styles and/or content, unlocking the potential of generating a wider range of creative images (Fig. 8).

For demonstrating this capacity, a crowd-source AMT evaluation is performed (Table 4), positioning PARASOL as the preferred method by users in terms of both content and style interpolation.

4.4.3 Textual Captions as Conditioning Inputs

Leveraging the multimodal properties of CLIP, content cues can be provided as either captions or images at sampling time. When a textual prompt is provided, our fine-tuned diffusion model is used for generating an image conditioned on its CLIP descriptor and an empty style descriptor. Using this generated image as content image y , the sampling procedure continues as described in Section 3.5.

The style cue can also be provided in textual format. The prompt can be encoded using CLIP and projected to a joint space through a pre-trained projector network [36]. By indexing all images in the “Style Database” S through ALADIN and projecting them to the joint feature space, a similar style image can be retrieved and used as input s to the sampling pipeline (Fig. 9).



Figure 9: Images generated from text prompts for both modalities. PARASOL accepts both visual and textual inputs for better transferring the user’s intent.

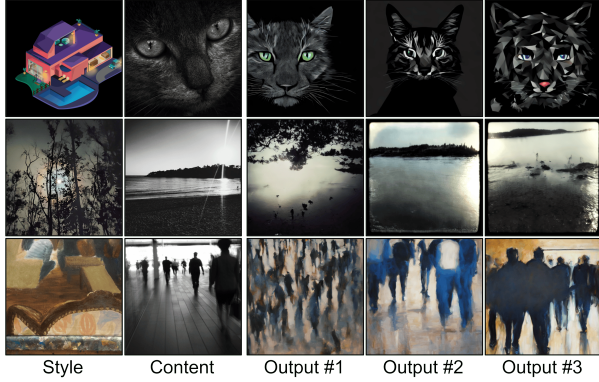


Figure 10: Diversity of fine-grained content. PARASOL can be used for synthesizing images with same semantics and fine-grained style yet diverse fine-grained content.

4.4.4 Content Diversity with Consistent Semantics

Although PARASOL is designed for preserving the fine-grained content details in y , it can also be extended for synthesizing images with consistent semantics and style yet diverse details and image layouts (Fig. 10).

Following a similar procedure to that in Section 4.4.3, an image can first be generated from y and used to guide the inversion process for transferring the semantics of y with new fine-grained content details.

4.5. Generative Visual Search

PARASOL can be applied for Generative Search, where search results are not constrained to a static corpus but fused with generation to yield images that more closely match a user’s search intent. Assuming an initial query in textual form, we use pre-existing text encoders (per Section 4.4.3) for CLIP and ALADIN to retrieve two sets of images that match their intent semantically and stylistically (Fig. 11, middle). The user picks images from each set, each of which may be interactively weighted to reflect their relevance to the users’ intent. Using the fine-grained interpolation method of Section 4.4.2, PARASOL is then used to generate an image which may either be accepted by the user or used as a further basis for semantic and style search. PARASOL thus provides a fine-grained way to disambiguate a single text prompt expressing a pair of modalities, and surface images beyond those available in a static text corpus.

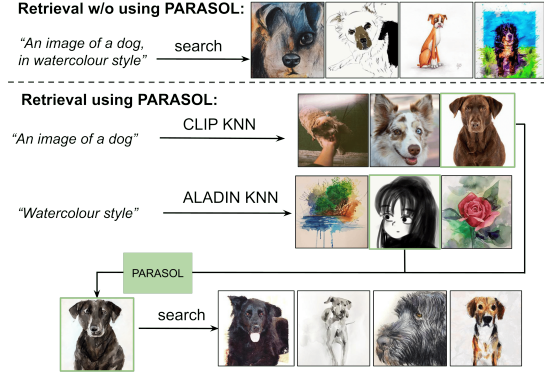


Figure 11: Generative Search. Our model can be used for aiding in image retrieval process (See Section 4.5).

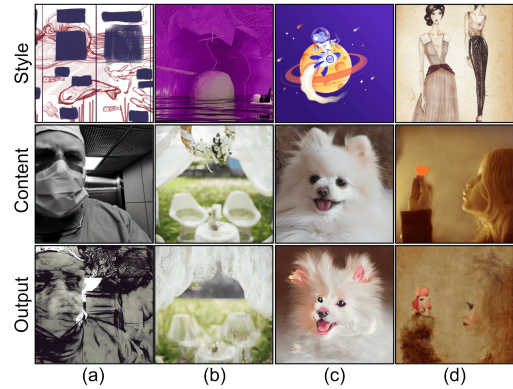


Figure 12: Failure cases - more details in Section 5.

5. Conclusion

We introduced PARASOL, a method for multimodal image synthesis with fine-grained parametric control over style leveraging the ALADIN embedding previously developed for style-based visual search. We show PARASOL may be applied to text, image or embedding conditioned generation enabling disentangled control over style and content at inference time. We also propose a novel method for obtaining paired data to train PARASOL leveraging cross-modal search. We show a use case in generative search, providing an image that can be used as a search query with more fine-grained properties.

Limitations The use of modality-specific encoders provides multiple benefits in terms of attribute disentanglement and parametric control, enabling interpolation and search. However, the representations they provide are not always fully disentangled, sometimes leading to artifacts and unwanted behaviours when generating new images (Fig. 12(c,d)). Another limitation is depicted in Fig. 12(a,b). When challenging styles or contents (e.g. faces) are provided to PARASOL, successful style transfer respecting the specific structure of the content can’t always be ensured. As such, future work can also explore other modalities such as sketch or segmentation maps to locally target regions [49] with fine-grained content and style cues.

References

- [1] Oron Ashual and Lior Wolf. Specifying object attributes and relations in interactive scene generation. In *The IEEE International Conference on Computer Vision (ICCV)*, October 2019.
- [2] Yogesh Balaji, Seungjun Nah, Xun Huang, Arash Vahdat, Jiaming Song, Karsten Kreis, Miika Aittala, Timo Aila, Samuli Laine, Bryan Catanzaro, Tero Karras, and Ming-Yu Liu. ediff-i: Text-to-image diffusion models with ensemble of expert denoisers. *arXiv preprint arXiv:2211.01324*, 2022.
- [3] Andreas Blattmann, Robin Rombach, Kaan Oktay, and Björn Ommer. Retrieval-augmented diffusion models, 2022.
- [4] Arantxa Casanova, Marlene Careil, Jakob Verbeek, Michal Drozdal, and Adriana Romero Soriano. Instance-conditioned gan. *Advances in Neural Information Processing Systems*, 34:27517–27529, 2021.
- [5] Haibo Chen, Zhizhong Wang, Huiming Zhang, Zhiwen Zuo, Ailin Li, Wei Xing, Dongming Lu, et al. Artistic style transfer with internal-external learning and contrastive learning. *Advances in Neural Information Processing Systems*, 34:26561–26573, 2021.
- [6] John Collomosse, Tu Bui, Michael J Wilber, Chen Fang, and Hailin Jin. Sketching with style: Visual search with sketches and aesthetic context. In *Proceedings of the IEEE international conference on computer vision*, pages 2660–2668, 2017.
- [7] Prafulla Dhariwal and Alexander Nichol. Diffusion models beat gans on image synthesis. *Advances in Neural Information Processing Systems*, 34:8780–8794, 2021.
- [8] Alexey Dosovitskiy, Lucas Beyer, Alexander Kolesnikov, Dirk Weissenborn, Xiaohua Zhai, Thomas Unterthiner, Mostafa Dehghani, Matthias Minderer, Georg Heigold, Sylvain Gelly, et al. An image is worth 16x16 words: Transformers for image recognition at scale. *arXiv preprint arXiv:2010.11929*, 2020.
- [9] Vincent Dumoulin, Jonathon Shlens, and Manjunath Kudlur. A learned representation for artistic style. *arXiv preprint arXiv:1610.07629*, 2016.
- [10] Oran Gafni, Adam Polyak, Oron Ashual, Shelly Sheynin, Devi Parikh, and Yaniv Taigman. Make-a-scene: Scene-based text-to-image generation with human priors. In *Computer Vision–ECCV 2022: 17th European Conference, Tel Aviv, Israel, October 23–27, 2022, Proceedings, Part XV*, pages 89–106. Springer, 2022.
- [11] Leon A Gatys, Alexander S Ecker, and Matthias Bethge. Image style transfer using convolutional neural networks. In *Proceedings of the IEEE conference on computer vision and pattern recognition*, pages 2414–2423, 2016.
- [12] Yunchao Gong, Liwei Wang, Micah Hodosh, Julia Hockenmaier, and Svetlana Lazebnik. Improving image-sentence embeddings using large weakly annotated photo collections. In *Computer Vision–ECCV 2014: 13th European Conference, Zurich, Switzerland, September 6–12, 2014, Proceedings, Part IV 13*, pages 529–545. Springer, 2014.
- [13] Shuyang Gu, Dong Chen, Jianmin Bao, Fang Wen, Bo Zhang, Dongdong Chen, Lu Yuan, and Baining Guo. Vector quantized diffusion model for text-to-image synthesis. In *Proceedings of the IEEE/CVF Conference on Computer Vision and Pattern Recognition*, pages 10696–10706, 2022.
- [14] Cusuh Ham, James Hays, Jingwan Lu, Krishna Kumar Singh, Zhifei Zhang, and Tobias Hinz. Modulating pre-trained diffusion models for multimodal image synthesis. *arXiv preprint arXiv:2302.12764*, 2023.
- [15] Cusuh Ham, Gemma Canet Tarrés, Tu Bui, James Hays, Zhe Lin, and John Collomosse. Cogs: Controllable generation and search from sketch and style. In *Computer Vision–ECCV 2022: 17th European Conference, Tel Aviv, Israel, October 23–27, 2022, Proceedings, Part XVI*, pages 632–650. Springer, 2022.
- [16] Jonathan Ho, Ajay Jain, and Pieter Abbeel. Denoising diffusion probabilistic models. *Advances in Neural Information Processing Systems*, 33:6840–6851, 2020.
- [17] Nisha Huang, Fan Tang, Weiming Dong, and Changsheng Xu. Draw your art dream: Diverse digital art synthesis with multimodal guided diffusion. In *Proceedings of the 30th ACM International Conference on Multimedia*, pages 1085–1094, 2022.
- [18] Xun Huang and Serge Belongie. Arbitrary style transfer in real-time with adaptive instance normalization. In *Proceedings of the IEEE international conference on computer vision*, pages 1501–1510, 2017.
- [19] Xun Huang, Arun Mallya, Ting-Chun Wang, and Ming-Yu Liu. Multimodal conditional image synthesis with product-of-experts gans. In *Computer Vision–ECCV 2022: 17th European Conference, Tel Aviv, Israel, October 23–27, 2022, Proceedings, Part XVI*, pages 91–109. Springer, 2022.
- [20] Justin Johnson, Agrim Gupta, and Li Fei-Fei. Image synthesis from reconfigurable layout and style. In *Proc. CVPR*, 2018.
- [21] Jacob Devlin Ming-Wei Chang Kenton and Lee Kristina Toutanova. Bert: Pre-training of deep bidirectional transformers for language understanding. In *Proceedings of naacl-HLT*, pages 4171–4186, 2019.
- [22] Diederik P Kingma and Max Welling. Auto-encoding variational bayes. *arXiv preprint arXiv:1312.6114*, 2013.
- [23] Benjamin Klein, Guy Lev, Gil Sadeh, and Lior Wolf. Fisher vectors derived from hybrid gaussian-laplacian mixture models for image annotation. *arXiv preprint arXiv:1411.7399*, 2014.
- [24] Svetlana Kutuzova, Oswin Krause, Douglas McCloskey, Mads Nielsen, and Christian Igel. Multimodal variational autoencoders for semi-supervised learning: In defense of product-of-experts. *arXiv preprint arXiv:2101.07240*, 2021.
- [25] Gihyun Kwon and Jong Chul Ye. Diffusion-based image translation using disentangled style and content representation. *arXiv preprint arXiv:2209.15264*, 2022.
- [26] Junnan Li, Dongxu Li, Caiming Xiong, and Steven Hoi. Blip: Bootstrapping language-image pre-training for unified vision-language understanding and generation. In *International Conference on Machine Learning*, pages 12888–12900. PMLR, 2022.
- [27] Yijun Li, Chen Fang, Jimei Yang, Zhaowen Wang, Xin Lu, and Ming-Hsuan Yang. Universal style transfer via feature transforms. *Advances in neural information processing systems*, 30, 2017.
- [28] Xuan Luo, Zhen Han, Lingfang Yang, and Lingling Zhang. Consistent style transfer. *arXiv preprint arXiv:2201.02233*, 2022.

- [29] Alex Nichol, Prafulla Dhariwal, Aditya Ramesh, Pranav Shyam, Pamela Mishkin, Bob McGrew, Ilya Sutskever, and Mark Chen. Glide: Towards photorealistic image generation and editing with text-guided diffusion models. *arXiv preprint arXiv:2112.10741*, 2021.
- [30] Dae Young Park and Kwang Hee Lee. Arbitrary style transfer with style-attentional networks. In *proceedings of the IEEE/CVF conference on computer vision and pattern recognition*, pages 5880–5888, 2019.
- [31] Alec Radford, Jong Wook Kim, Chris Hallacy, Aditya Ramesh, Gabriel Goh, Sandhini Agarwal, Girish Sastry, Amanda Askell, Pamela Mishkin, Jack Clark, et al. Learning transferable visual models from natural language supervision. In *International conference on machine learning*, pages 8748–8763. PMLR, 2021.
- [32] Colin Raffel, Noam Shazeer, Adam Roberts, Katherine Lee, Sharan Narang, Michael Matena, Yanqi Zhou, Wei Li, and Peter J Liu. Exploring the limits of transfer learning with a unified text-to-text transformer. *The Journal of Machine Learning Research*, 21(1):5485–5551, 2020.
- [33] Aditya Ramesh, Prafulla Dhariwal, Alex Nichol, Casey Chu, and Mark Chen. Hierarchical text-conditional image generation with clip latents. *arXiv preprint arXiv:2204.06125*, 2022.
- [34] Robin Rombach, Andreas Blattmann, Dominik Lorenz, Patrick Esser, and Björn Ommer. High-resolution image synthesis with latent diffusion models. In *Proceedings of the IEEE/CVF Conference on Computer Vision and Pattern Recognition*, pages 10684–10695, 2022.
- [35] Robin Rombach, Andreas Blattmann, and Björn Ommer. Text-guided synthesis of artistic images with retrieval-augmented diffusion models. *arXiv preprint arXiv:2207.13038*, 2022.
- [36] Dan Ruta, Andrew Gilbert, Pranav Aggarwal, Naveen Marri, Ajinkya Kale, Jo Briggs, Chris Speed, Hailin Jin, Baldo Faieta, Alex Filipkowski, et al. Stylelabel: Artistic style tagging and captioning. In *Computer Vision–ECCV 2022: 17th European Conference, Tel Aviv, Israel, October 23–27, 2022, Proceedings, Part VIII*, pages 219–236. Springer, 2022.
- [37] Dan Ruta, Saeid Motiian, Baldo Faieta, Zhe Lin, Hailin Jin, Alex Filipkowski, Andrew Gilbert, and John Collomosse. Aladin: all layer adaptive instance normalization for fine-grained style similarity. In *Proceedings of the IEEE/CVF International Conference on Computer Vision*, pages 11926–11935, 2021.
- [38] Chitwan Saharia, William Chan, Saurabh Saxena, Lala Li, Jay Whang, Emily Denton, Seyed Kamyar Seyed Ghasemipour, Burcu Karagol Ayan, S Sara Mahdavi, Rapha Gontijo Lopes, et al. Photorealistic text-to-image diffusion models with deep language understanding. *arXiv preprint arXiv:2205.11487*, 2022.
- [39] Tamar Rott Shaham, Tali Dekel, and Tomer Michaeli. Singan: Learning a generative model from a single natural image. In *Proceedings of the IEEE/CVF International Conference on Computer Vision*, pages 4570–4580, 2019.
- [40] Lu Sheng, Ziyi Lin, Jing Shao, and Xiaogang Wang. Avatar-net: Multi-scale zero-shot style transfer by feature decoration. In *Proceedings of the IEEE conference on computer vision and pattern recognition*, pages 8242–8250, 2018.
- [41] Shelly Sheynin, Oron Ashual, Adam Polyak, Uriel Singer, Oran Gafni, Eliya Nachmani, and Yaniv Taigman. Knn-diffusion: Image generation via large-scale retrieval. *arXiv preprint arXiv:2204.02849*, 2022.
- [42] Yuge Shi, Brooks Paige, Philip Torr, et al. Variational mixture-of-experts autoencoders for multi-modal deep generative models. *Advances in Neural Information Processing Systems*, 32, 2019.
- [43] Wei Sun and Tianfu Wu. Image synthesis from reconfigurable layout and style. In *Proceedings of the IEEE/CVF International Conference on Computer Vision*, pages 10531–10540, 2019.
- [44] Tristan Sylvain, Pengchuan Zhang, Yoshua Bengio, R Devon Hjelm, and Shikhar Sharma. Object-centric image generation from layouts. In *Proceedings of the AAAI Conference on Artificial Intelligence*, volume 35, pages 2647–2655, 2021.
- [45] Michael J Wilber, Chen Fang, Hailin Jin, Aaron Hertzmann, John Collomosse, and Serge Belongie. Bam! the behance artistic media dataset for recognition beyond photography. In *Proceedings of the IEEE international conference on computer vision*, pages 1202–1211, 2017.
- [46] Michael J. Wilber, Chen Fang, Hailin Jin, Aaron Hertzmann, John P. Collomosse, and Serge J. Belongie. Bam! the behance artistic media dataset for recognition beyond photography. *CoRR*, abs/1704.08614, 2017.
- [47] Mike Wu and Noah Goodman. Multimodal generative models for scalable weakly-supervised learning. *Advances in neural information processing systems*, 31, 2018.
- [48] Weihao Xia, Yujiu Yang, Jing-Hao Xue, and Baoyuan Wu. Tedigan: Text-guided diverse face image generation and manipulation. In *Proceedings of the IEEE/CVF conference on computer vision and pattern recognition*, pages 2256–2265, 2021.
- [49] Yu Zeng, Zhe Lin, Jianming Zhang, Qing Liu, John Collomosse, Jason Kuen, and Vishal M Patel. Scenecomposer: Any-level semantic image synthesis. *arXiv preprint arXiv:2211.11742*, 2022.
- [50] Kai Zhang, Nick Kolkin, Sai Bi, Fujun Luan, Zexiang Xu, Eli Shechtman, and Noah Snavely. Arf: Artistic radiance fields. In *Computer Vision–ECCV 2022: 17th European Conference, Tel Aviv, Israel, October 23–27, 2022, Proceedings, Part XXXI*, pages 717–733. Springer, 2022.
- [51] Lvmin Zhang and Maneesh Agrawala. Adding conditional control to text-to-image diffusion models. *arXiv preprint arXiv:2302.05543*, 2023.
- [52] Richard Zhang, Phillip Isola, Alexei A Efros, Eli Shechtman, and Oliver Wang. The unreasonable effectiveness of deep features as a perceptual metric. In *Proceedings of the IEEE conference on computer vision and pattern recognition*, pages 586–595, 2018.
- [53] Yuxin Zhang, Fan Tang, Weiming Dong, Haibin Huang, Chongyang Ma, Tong-Yee Lee, and Changsheng Xu. Domain enhanced arbitrary image style transfer via contrastive learning. In *ACM SIGGRAPH 2022 Conference Proceedings*, pages 1–8, 2022.
- [54] Bo Zhao, Lili Meng, Weidong Yin, and Leonid Sigal. Image generation from layout. In *Proceedings of the IEEE/CVF Conference on Computer Vision and Pattern Recognition*, pages 8584–8593, 2019.
- [55] Ye Zhu, Yu Wu, Kyle Olszewski, Jian Ren, Sergey Tulyakov, and Yan Yan. Discrete contrastive diffusion for cross-modal music and image generation. In *The Eleventh International Conference on Learning Representations*.

A. Training Supervision Data

In order to obtain suitable data for training our model, a set of 500k triplets (output image x , content image y , style image s) is obtained through cross-modal search (See Section 3.1 for details). The process in which these images are obtained ensures a certain disentanglement between content in x and s and between style in x and y . These triplets are essential for the training of PARASOL and assist in disentangling the two attributes in which the network is conditioned. Fig. 13 shows a few examples of such triplets.

B. Baselines Comparison

Quantitative and qualitative evaluations are provided in the main paper comparing PARASOL to several image generation and neural style transfer (NST) methods (See Tables 1 and 2). A visualization of the most competitive methods is also provided in Fig. 3. In this section, we provide a visualization of all methods (Fig. 14).

The figure shows how RDM [3] and ControlNet [51] are the methods that less accurately keep the fine-grained style and control details. RDM encodes both conditions using the same kind of encoding, without encouraging any disentanglement, leading to confusion of the network in which attributes should be transferred from each input condition. For the comparison, ControlNet was trained following the author’s indications and using our set of triplets as training data. It only accepts content information given in textual format, so we use automatically generated captions from each content image y using BLIP [26]. Thus, the method was trained by feeding the generated captions as input and the style images as a conditioning that needs to be learnt. Their paper shows the method is able to learn a wide range of conditioning signals including sketches, segmentation maps and edgemaps. It doesn’t, however, show any example in which the conditioning signal is not structure-based. Therefore, we hypothesize the architecture or parameters of ControlNet might not be suitable for successfully accommodating a condition such as style.

i. Comparison to eDiff-I

eDiff-I [2] is a diffusion-based method that generates images from text. It conditions the generation process on T5 text embeddings [32], CLIP image embeddings and CLIP text embeddings [31]. The use of CLIP image embeddings allows extending the method for style transfer from a reference style image.

This work wasn’t included in the previous baseline comparison due to lack of open source code or public pre-trained models. However, we show in Fig. 15 a visual comparison to a set of synthetic images they provide. Those images were generated by eDiff-I from long descriptive captions and the displayed style images. They also provide unstylized images generated from the same descriptions without conditioning on any style. eDiff-I incorporates T5 text embeddings in their pipeline, allowing it to process much

more complex text prompts than those that can be encoded through CLIP. Therefore, in our comparison, we consider as content input the provided unstylized synthetic images generated from the same prompts.

C. Amazon Mechanical Turk Experiments

The results of 8 different Amazon Mechanical Turk (AMT) experiments were presented in the main paper, 6 of them comparing our method to different baselines in terms of style, content and overall preference (Section 4.2) and 2 comparing style and content interpolations to DiffuseIT [25] and RDM [3] (Section 4.4.2).

In particular, the instructions given to the workers in each task were the following:

- Image generation preference in terms of style: *"The photo has been transformed into the style of the artwork in multiple ways. Study the options and pick which most closely resembles the style of the artwork whilst also keeping the most structure detail in the photo."*
- Image generation preference in terms of content: *"The photo has been transformed into the style of the artwork in multiple ways. Study the options and pick which keeps the best structure of the content, from details in the content image."*
- Image generation overall preference: *"The photo has been transformed into the style of the artwork in multiple ways. Study the options and pick which most closely resembles the style of the artwork whilst also keeping the most structure detail in the photo."*
- Preferred method for content interpolation: *"These images have been generated by interpolating Photo1 and Photo2 and transferring the style of the Artwork. Study the options and pick which set of images better display a smooth transition from content/semantics of Photo1 and Photo2 while maintaining good image quality and a consistent style similar to the Artwork."*
- Preferred method for style interpolation: *"These images have been generated considering the structure in the Content image and an interpolation of styles from both Artworks. Study the options and pick which set of images better display a smooth transition from the style of Artwork1 to Artwork2 while maintaining good image quality and a consistent structure similar to the Content image."*

The first three instructions were used for separately comparing PARASOL to image generation methods and NST ones. A few examples of the images shown to the users in the AMT interpolation experiments are shown in Figs. 16 and 17.

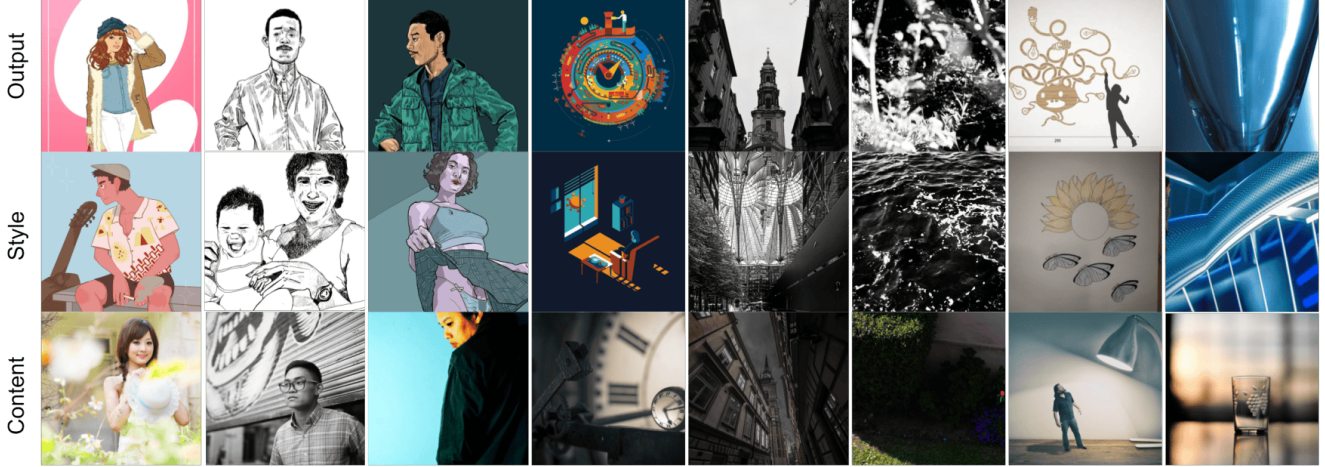


Figure 13: Visualization of triplets used for training our model. These triplets contain: output image x , similar image in terms of style s and similar image in terms of content y . During training, the method learns to reconstruct x by conditioning on y and s .

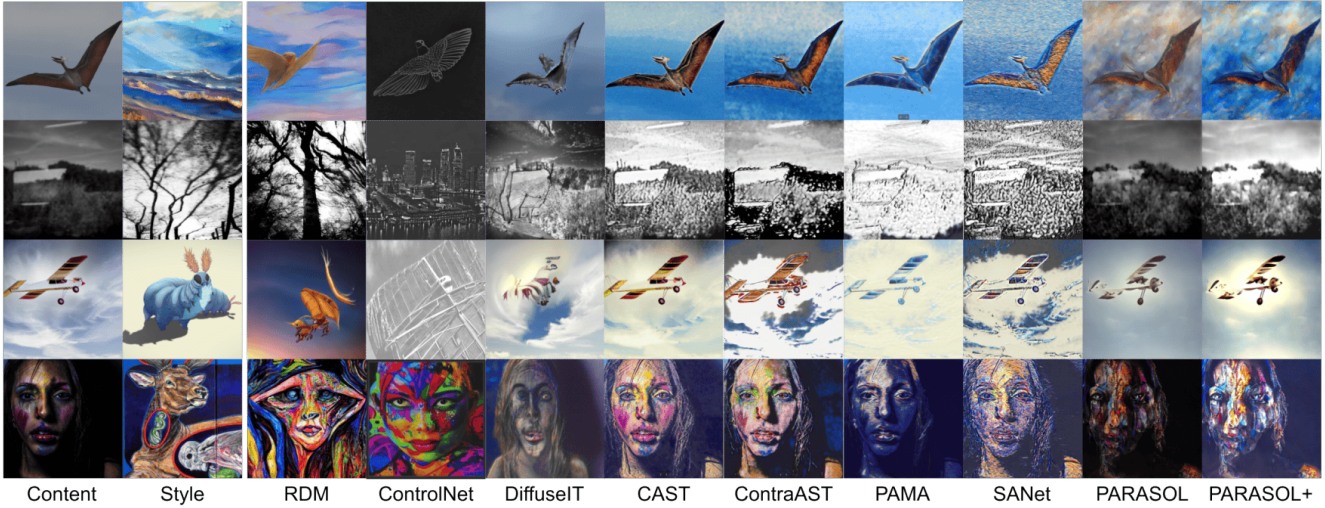


Figure 14: Baselines Comparison. Visualization of PARASOL, PARASOL+ and all image generation (RDM [3], ControlNet [51], DiffuseIT [25]) and NST methods (CAST [53], ContraAST [5], PAMA [28], SANet [30]) to which we compare.

D. Generative Search

Briefly introduced in Section 4.5, generative search is presented as one of the main applications for our model. Fig. 18 shows a different example of how PARASOL can be used for either refining the search with a more fine-grained query in terms of style and semantics or for generating a synthetic image that closely matches the user’s intent. As depicted in this example, style and/or content properties of different existent images can be combined for a more fine-grained search.

E. Additional Visualization Examples

We provide a few examples of images generated by transferring famous styles (Fig. 19) and additional visual-

ization examples for all experiments in Section 4.4.

i. Images Generated from Textual Inputs

An example of images generated with PARASOL using textual vs. image inputs for style and/or content is provided in Fig. 20.

ii. Images Generated with Different Lambda Values

PARASOL offers control in the amount of fine-grained content details that should be kept in the generated image vs. how much the image should be adapted to the new style. This can be controlled via the parameter λ (Fig. 21).



Figure 15: Comparison to eDiff-I [2]. PARASOL closely transfers the fine-grained style of the style image while keeping the fine-grained details and structure of the content image. The concept of style, however, slightly differs between both works. While eDiff-I understands "style" as a collection of colours and structure in which the information should be presented, PARASOL focuses on the type of artistic style (e.g. oil painting, illustration...) and its fine-grained details such as types of brush strokes, while also transferring the overall colour tonalities.

iii. Images Generated with Different Classifier-Free Guidance Parameters

The classifier-free guidance parameters g_s and g_y indicate how much weight the style s and content y conditions should have in the generation of the new image. Fig. 22 visualizes the difference those values can make in the generated samples.

iv. Images Generated by combining Different Lambda Values and Classifier-Free Guidance Parameters

Fig. 23 shows images generated by considering different pairs of g_s and λ values, while keeping g_y constant. The ratio of these two parameters defines how much creativity the model is allowed to introduce in the structure and stylization of the image.

v. Images Generated with Style and Content Interpolation

PARASOL allows the generation of images from a combination of different styles and/or contents (Figs. 24 and 25). For combining the information from each pair of descriptors, their spherical interpolation is computed, considering a parameter $0 \leq \alpha \leq 1$. If $\alpha = 0$ only the first descriptor is considered, while $\alpha = 1$ indicates the second descriptor is the only one taken into account.

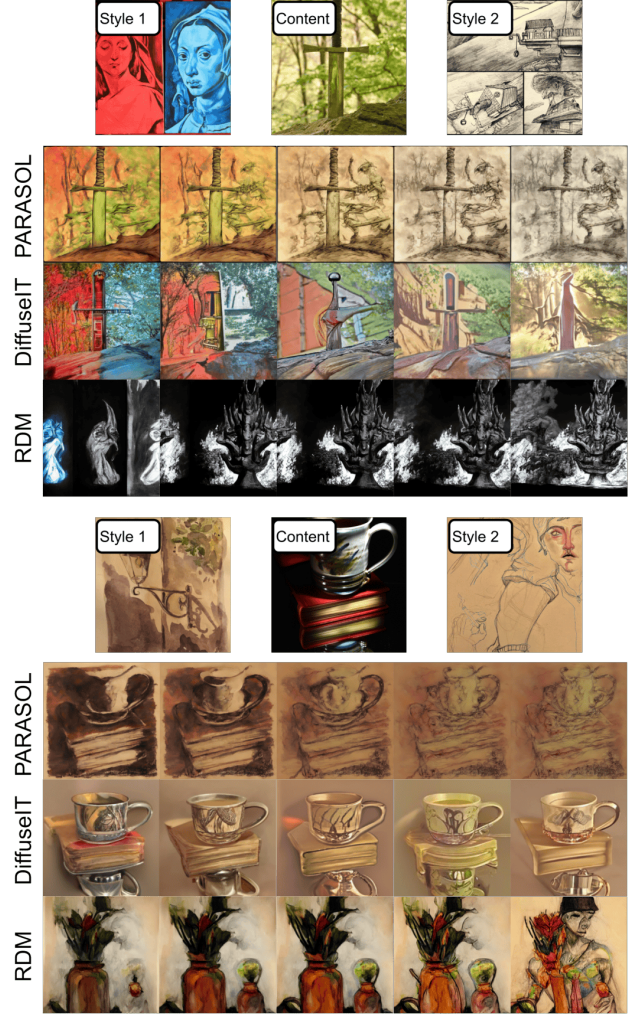


Figure 16: Baseline comparison for style interpolation. Visualization of images generated by PARASOL, DiffuseIT and RDM using interpolation between "Style 1" and "Style 2".

a) Style interpolation

The use of a parametric model [37] for encoding the style condition allows the synthesis of images by interpolating different styles. The nuanced information this model is capable to encode allows the interpolation of very similar styles (Fig. 26) while also being able to interpolate more different styles (Fig. 27).

b) Content Interpolation

We encode the content information using CLIP [31] which is also a parametric model. Therefore, not only PARASOL can generate images by interpolating different styles, but it also allows the interpolation of different content information. The content information being interpolated can con-

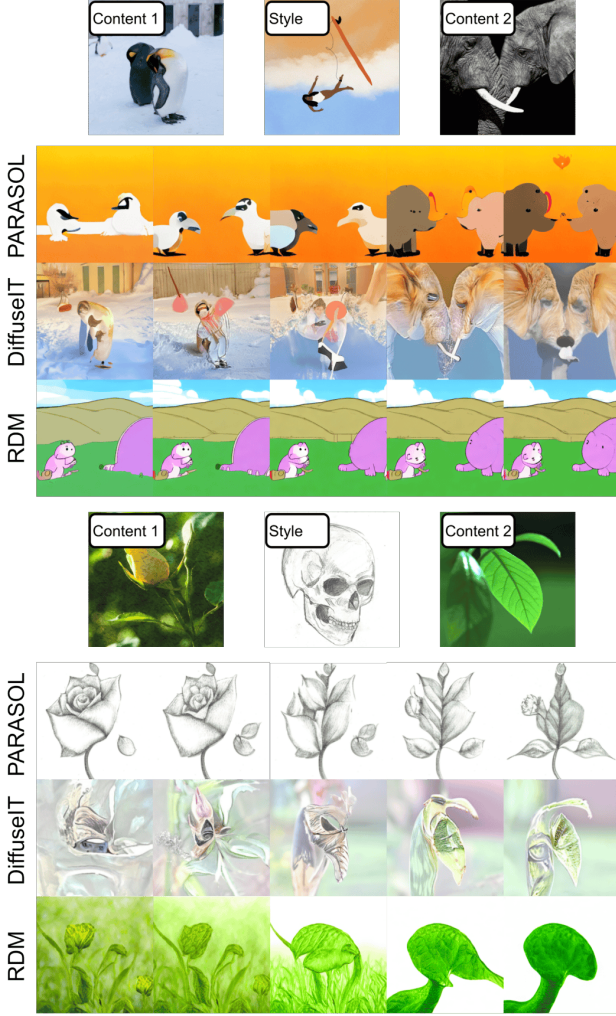


Figure 17: Baseline comparison for content interpolation. Visualization of images generated by PARASOL, DiffuseIT and RDM using interpolation between "Content 1" and "Content 2".

tain similar semantics (Fig. 28) or different ones (Fig. 29).

vi. Images Generated with Different Fine-Grained Content Details

Section 4.4.4 details how PARASOL can generate images with consistent semantics and fine-grained style while offering diversity in the fine-grained content details. Fig. 30 offers examples of this use case using $\lambda = 20$, $g_s = 5$ and $g_y = 5$. However, those parameters could be tuned for further control over the attributes of the final image.

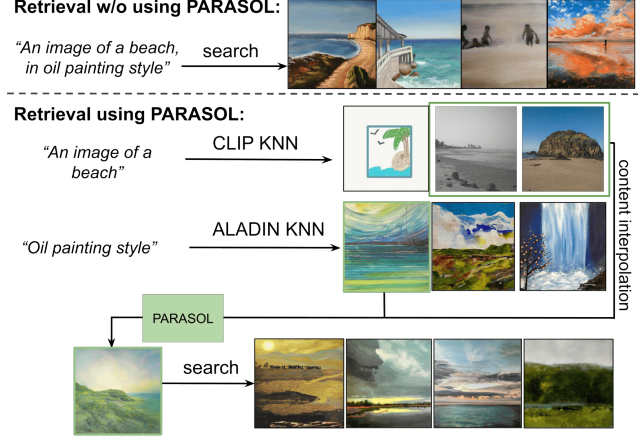


Figure 18: Use case for Generative Search. All PARASOL controllability tools, including interpolation capability, can be leveraged for obtaining a fine-grained query to refine the search and more closely match the user's intent.



Figure 19: PARASOL Generated Images. Images generated using PARASOL, by transferring the style of famous paintings into different landmarks and scenery images.

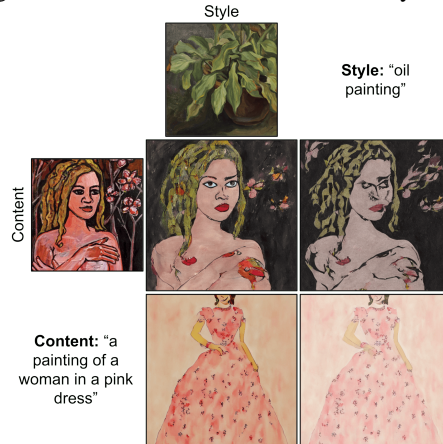


Figure 20: Images generated using different combinations of textual and visual inputs for content and style. While providing an image to describe intended content or style provides more fine-grained details, textual inputs allow useful descriptions and unlimited creativity.

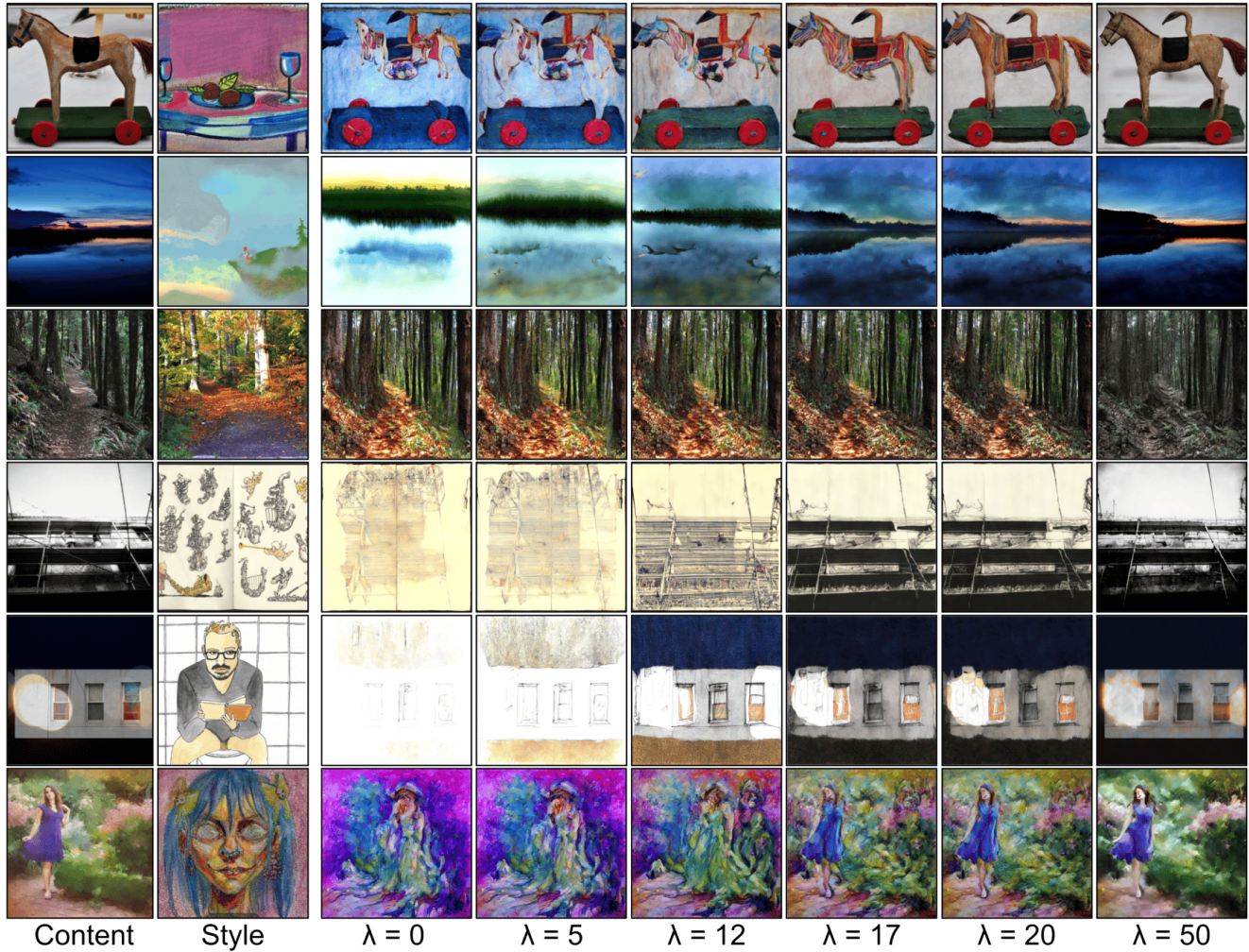


Figure 21: Images generated with different λ values. Higher values of lambda lead to more faithfulness in the structure and fine-grained details from the content input. Low lambda values lead to more stylised images that allow more creative structures and flexibility in fine-grained content details. In this example, $T = 50$, meaning lambda can take values from 0 to 50.

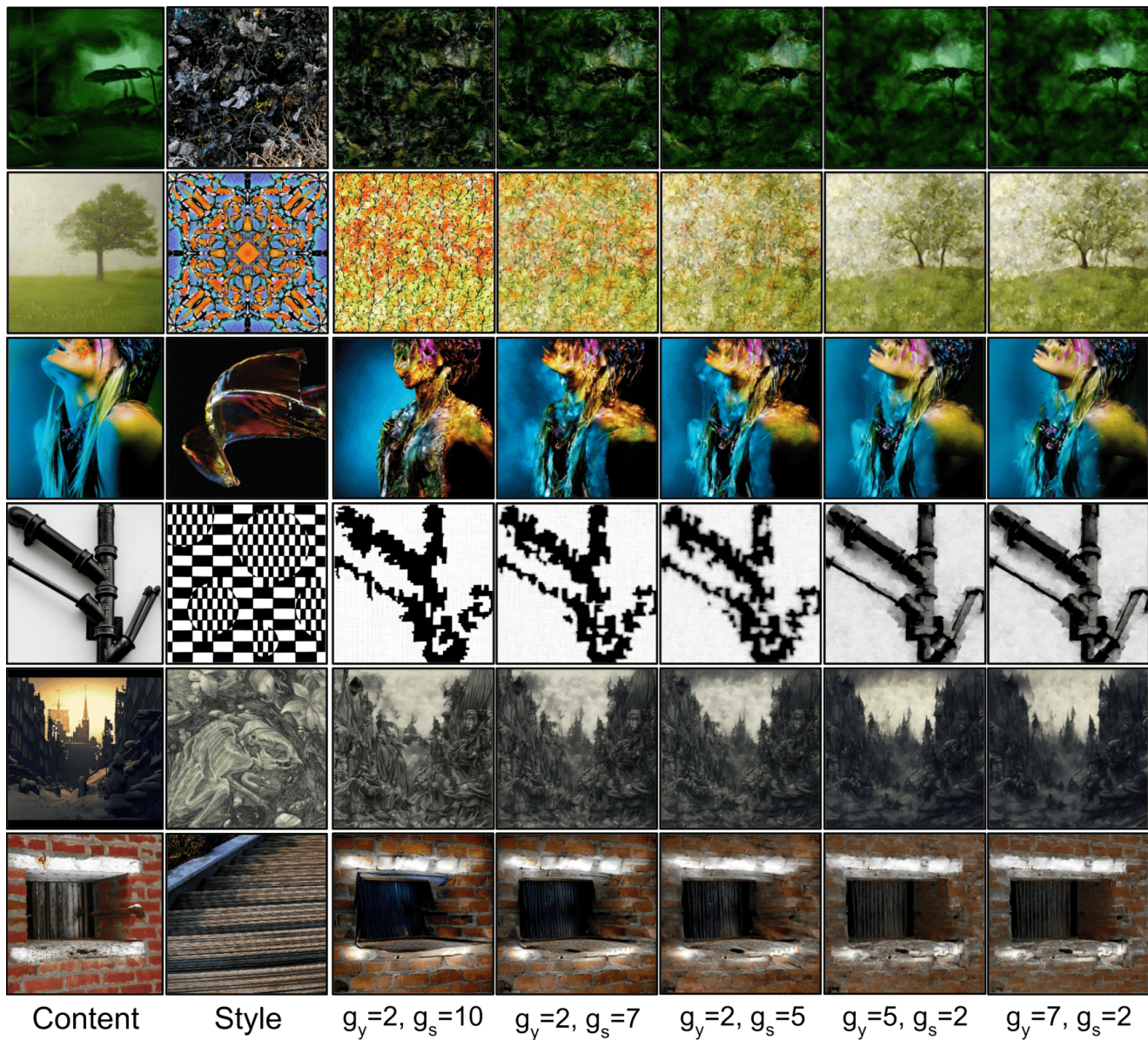


Figure 22: Images generated by PARASOL using different values for g_s and g_y . Fixing λ means that the structure of the content image is preserved in the same degree for all images. However, the balance between preserved semantics and style change with the ratio of both parameters.

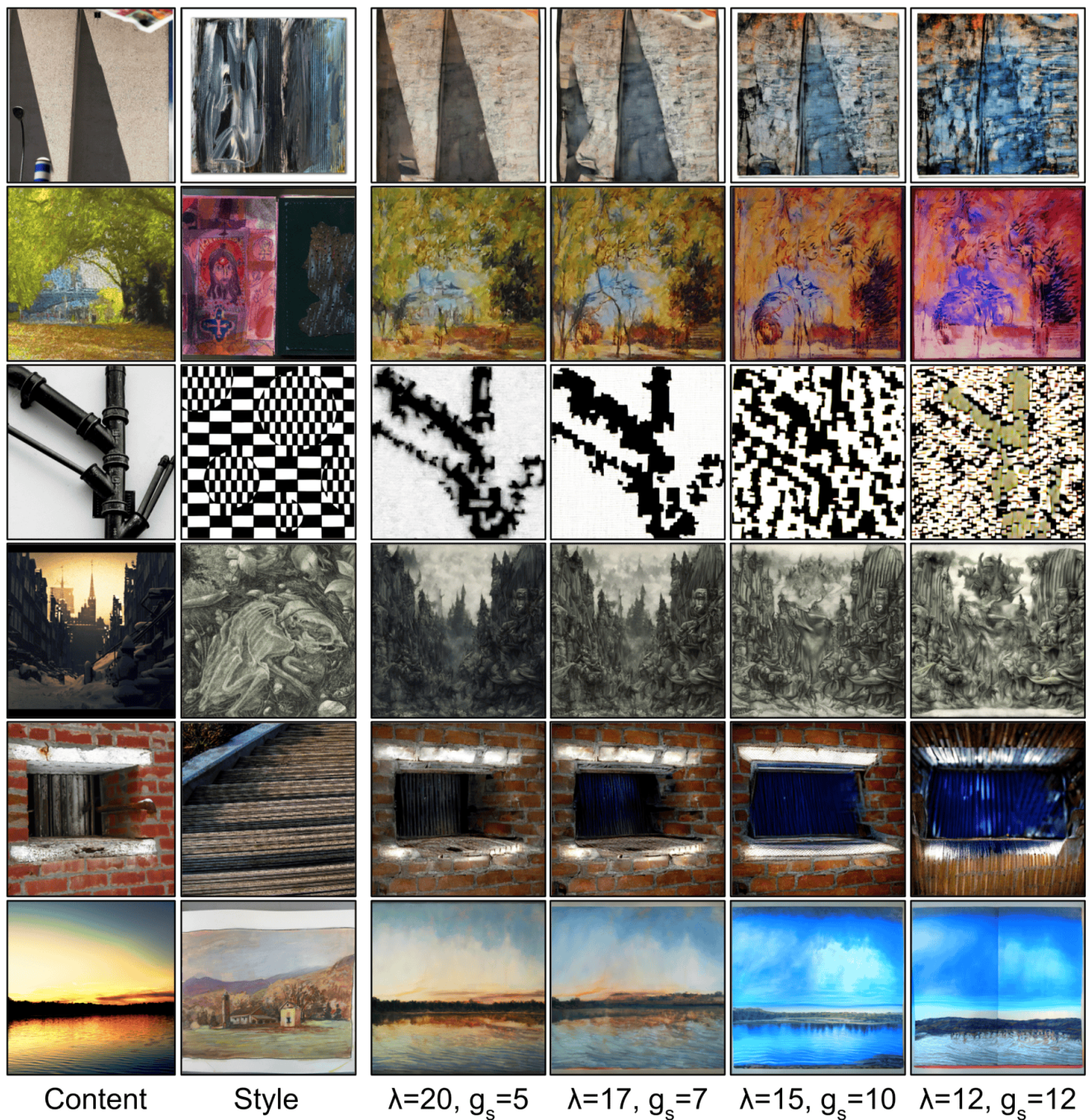


Figure 23: Images generated by PARASOL using different values for λ and g_s . High values of λ paired with low g_s lead to more faithful structures to the content input with more subtle stylization, while high values of g_s and low λ values lead to a more noticeable influence of the style image, with more space for creativity in terms of content details. The combination of both parameters allows for a wider range of options in terms of fine-grained controllability of the style and content details in the output image.

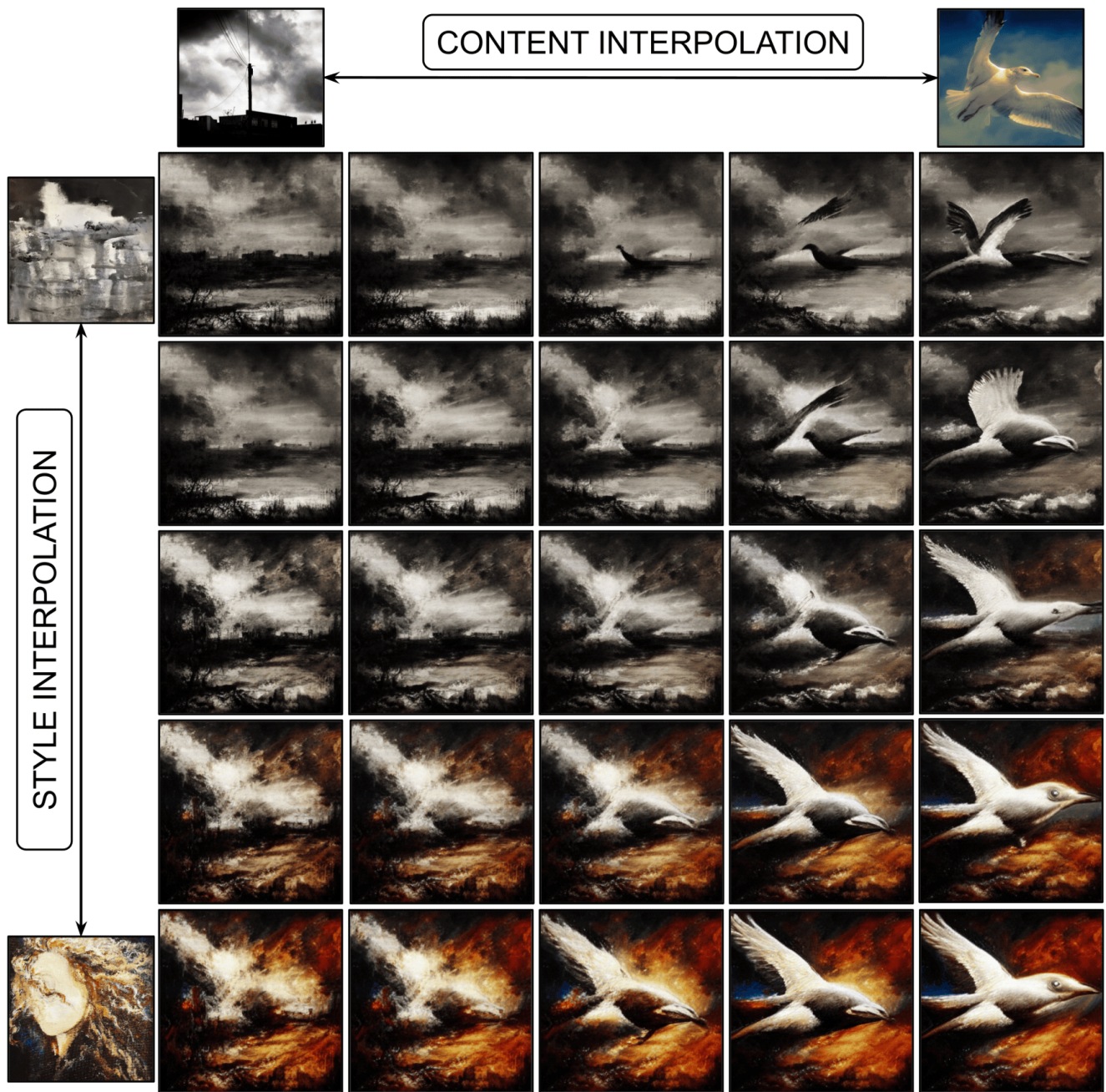


Figure 24: Style and Content interpolations. Visualization of different degrees of interpolation between two content images and two styles. For both style and content interpolations, values $\alpha = 0, 0.25, 0.5, 0.75, 1$ are considered.

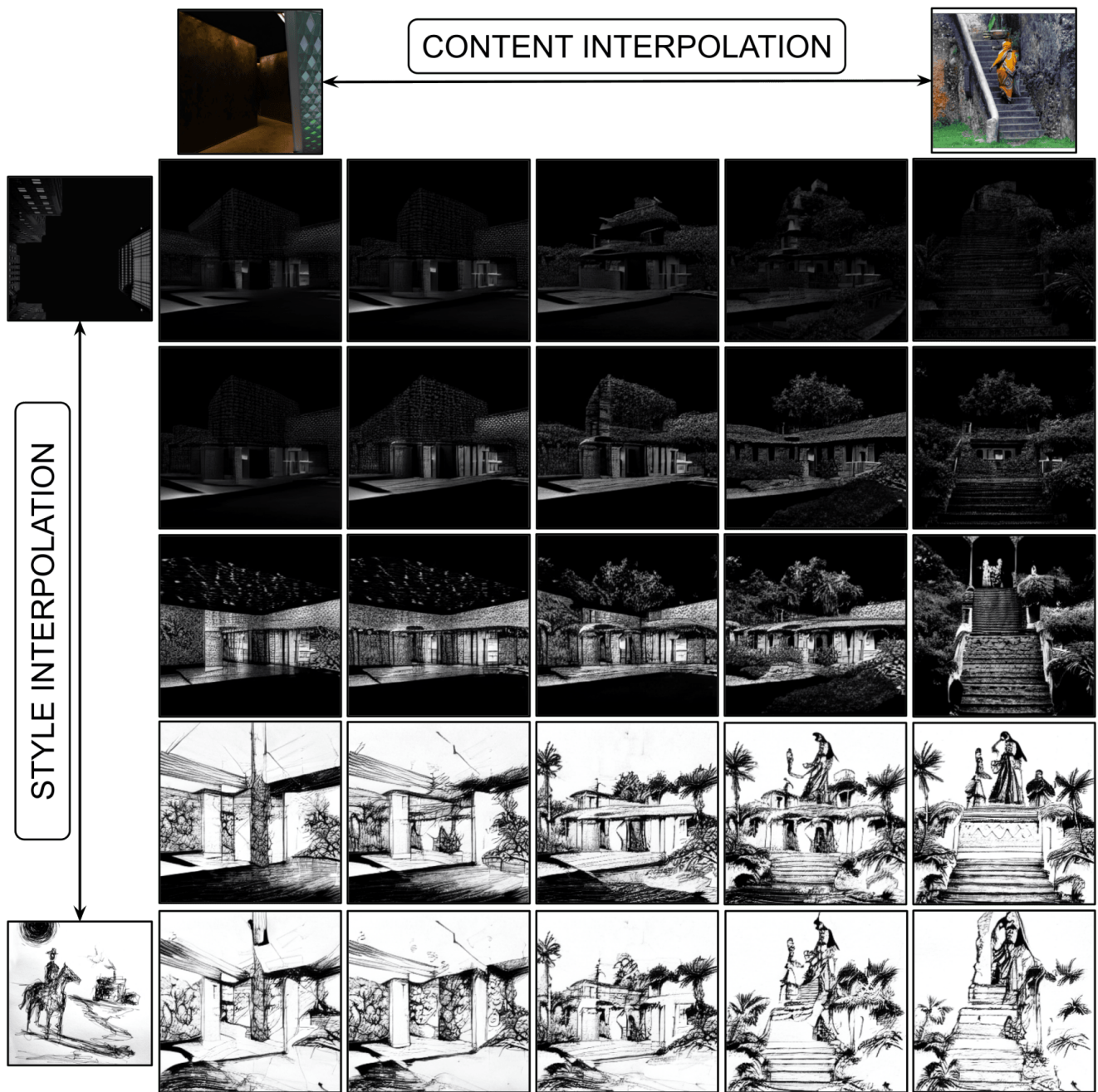


Figure 25: Style and Content interpolations. Second example of images generated by interpolating two content images and two styles in different degrees. For both style and content interpolations, values $\alpha = 0, 0.25, 0.5, 0.75, 1$ are considered.

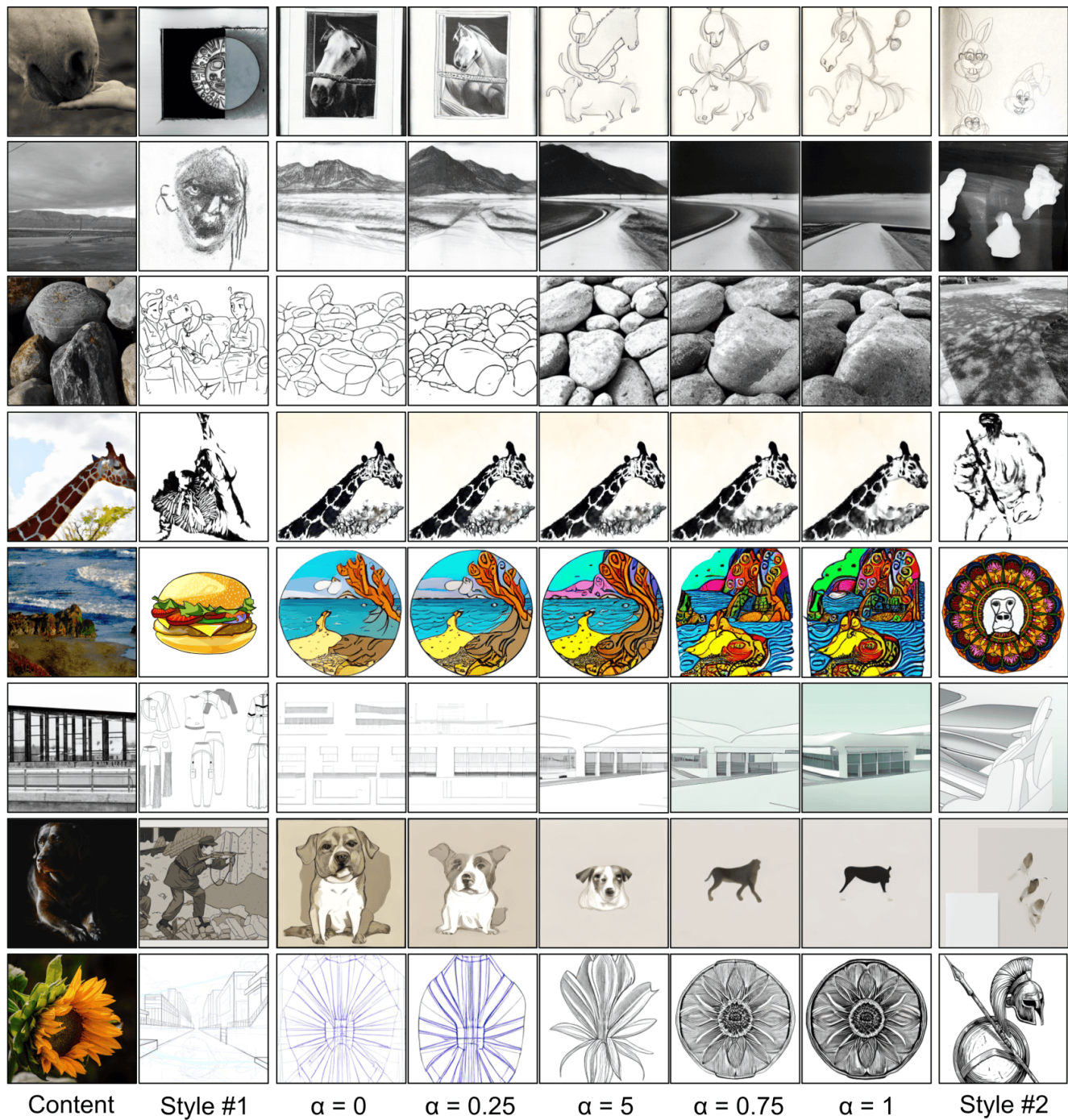


Figure 26: Style interpolation with similar fine-grained styles. Images generated by conditioning on a content image and different interpolations of two very similar styles, transferring and combining their nuances and particular characteristics.

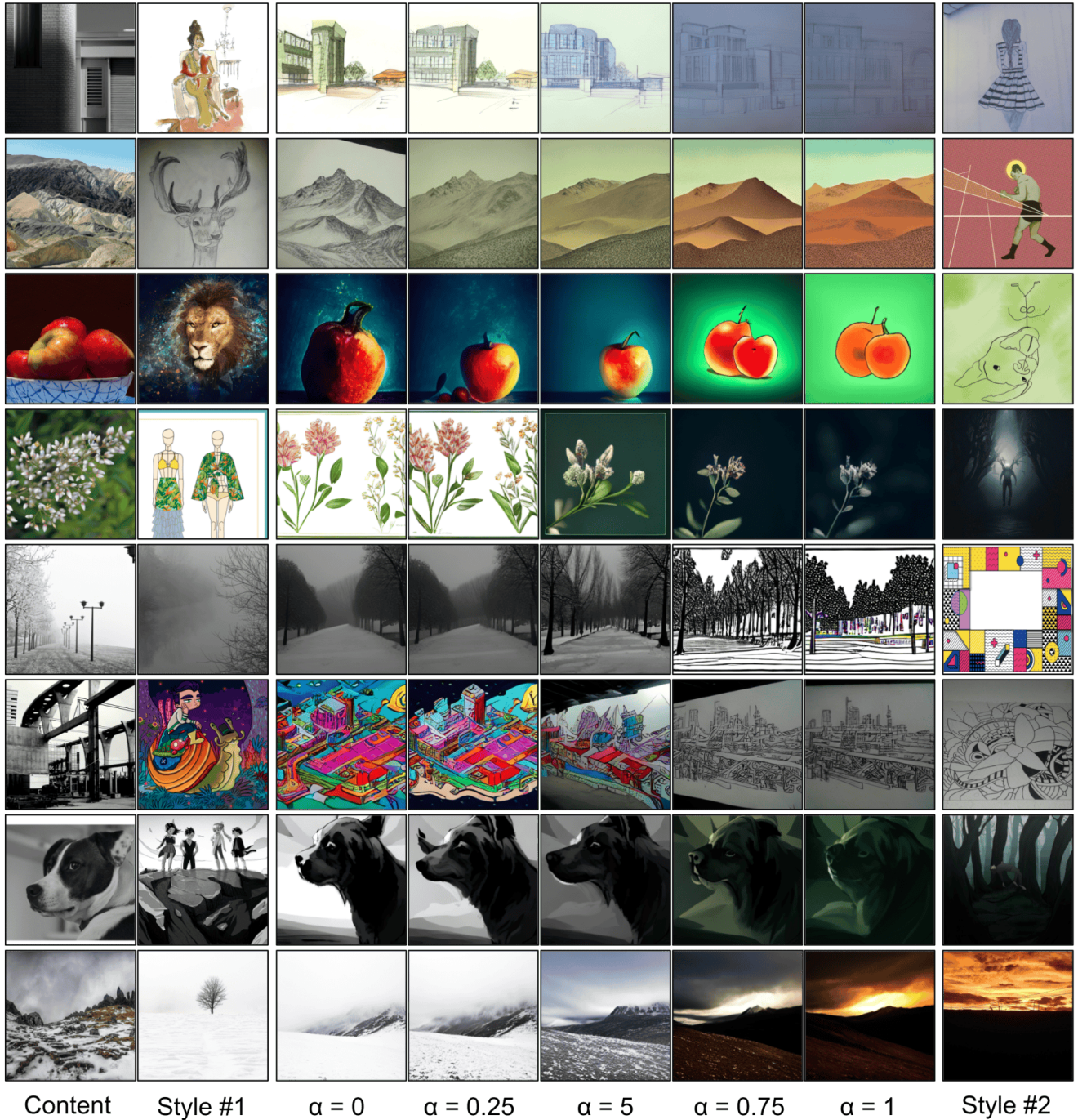


Figure 27: Style interpolation with visually different styles. Images generated by conditioning on a content image and different interpolations of two significantly different styles. PARASOL is able to smoothly transition between both styles, demonstrating its creative capabilities.

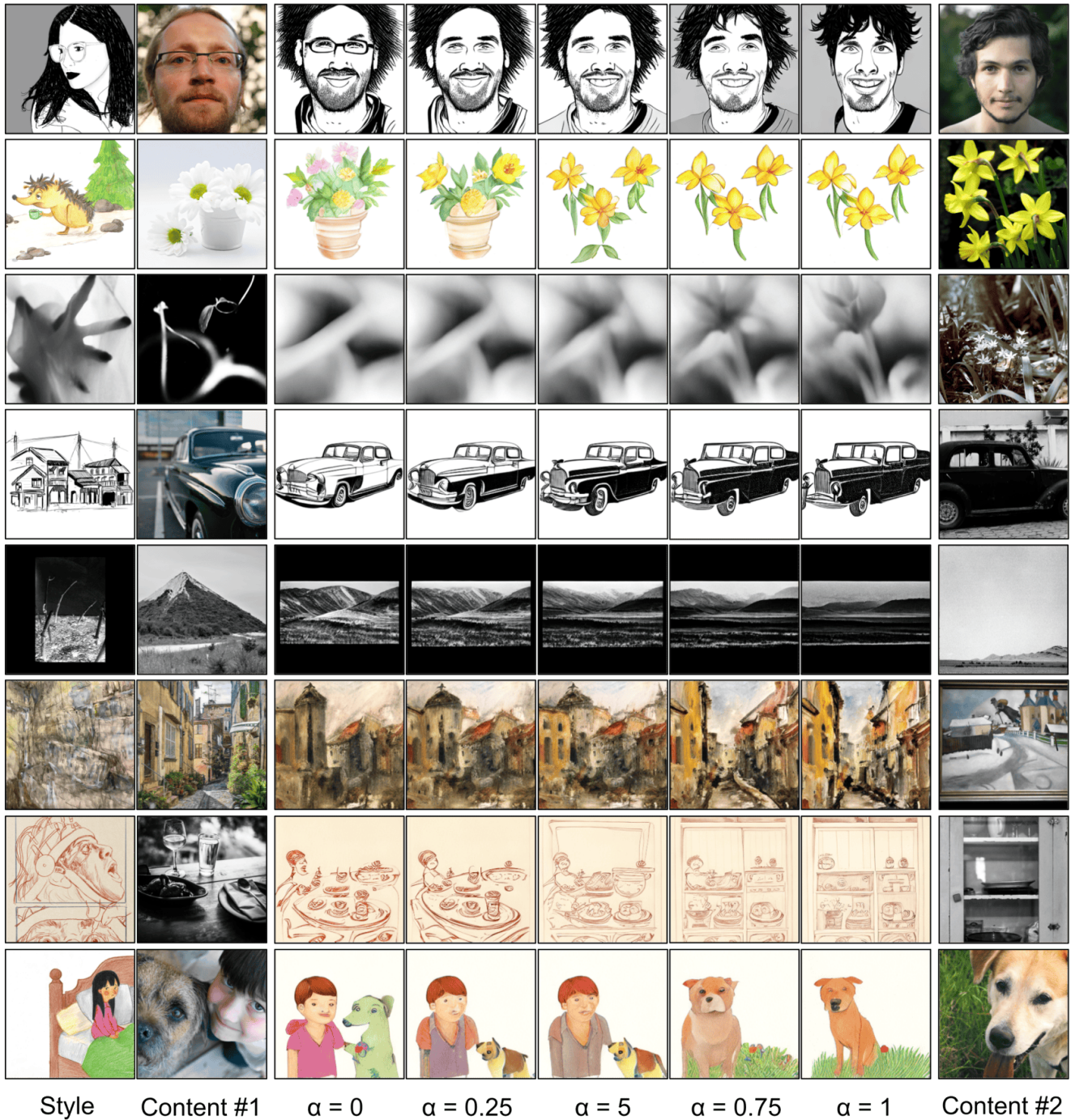


Figure 28: Content interpolation with similar semantics. Images generated by conditioning on a style and content information corresponding to the interpolation of two signals with similar semantics. PARASOL can capture the nuances and fine-grained details of each content input and combine them for generating brand new images.

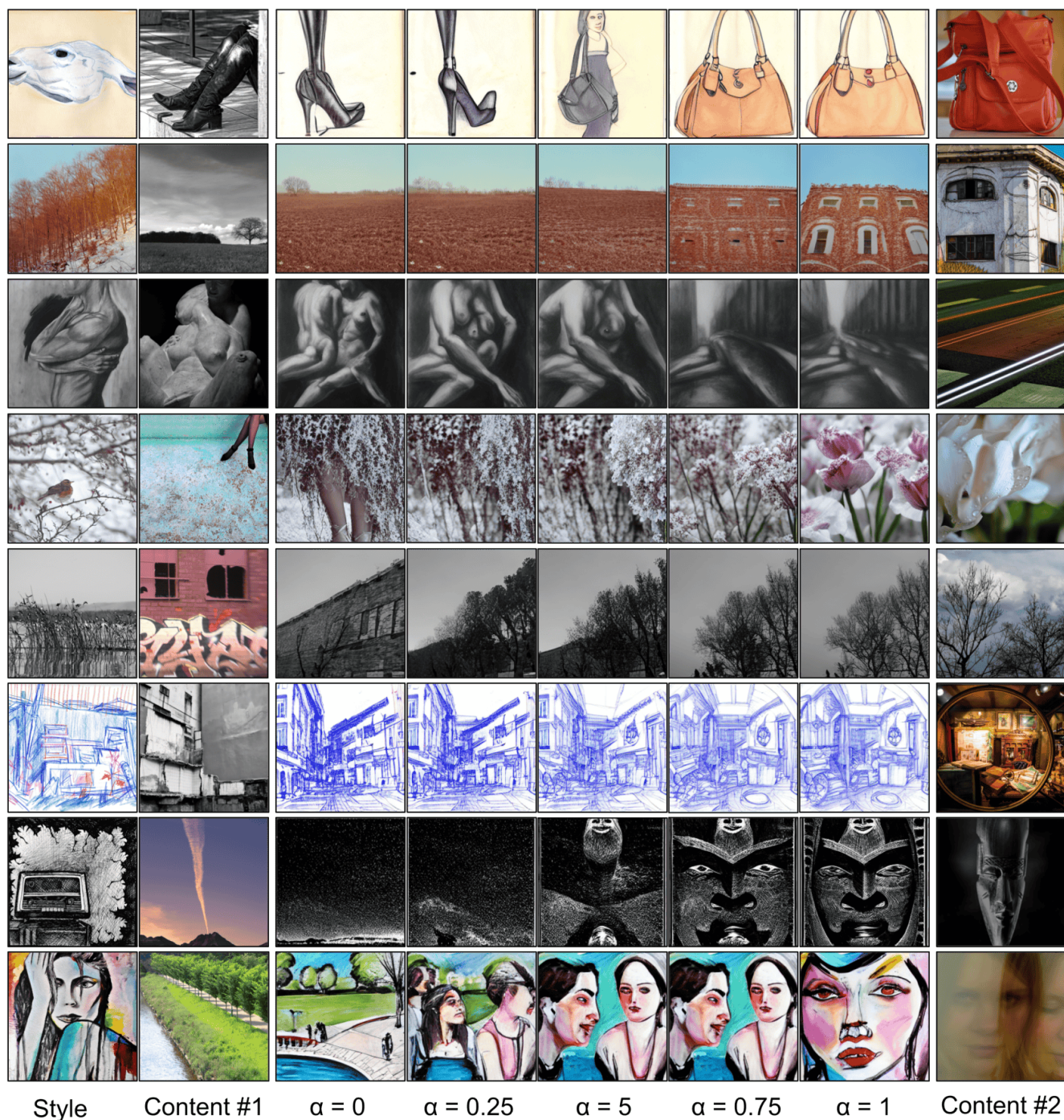


Figure 29: Content interpolation combining different semantics. Images generated by conditioning on a style and content information coming from the interpolation of two signals with different semantics. PARASOL can consistently transfer the style to both scenes or elements and combine them in a smooth way without losing image quality or realism.

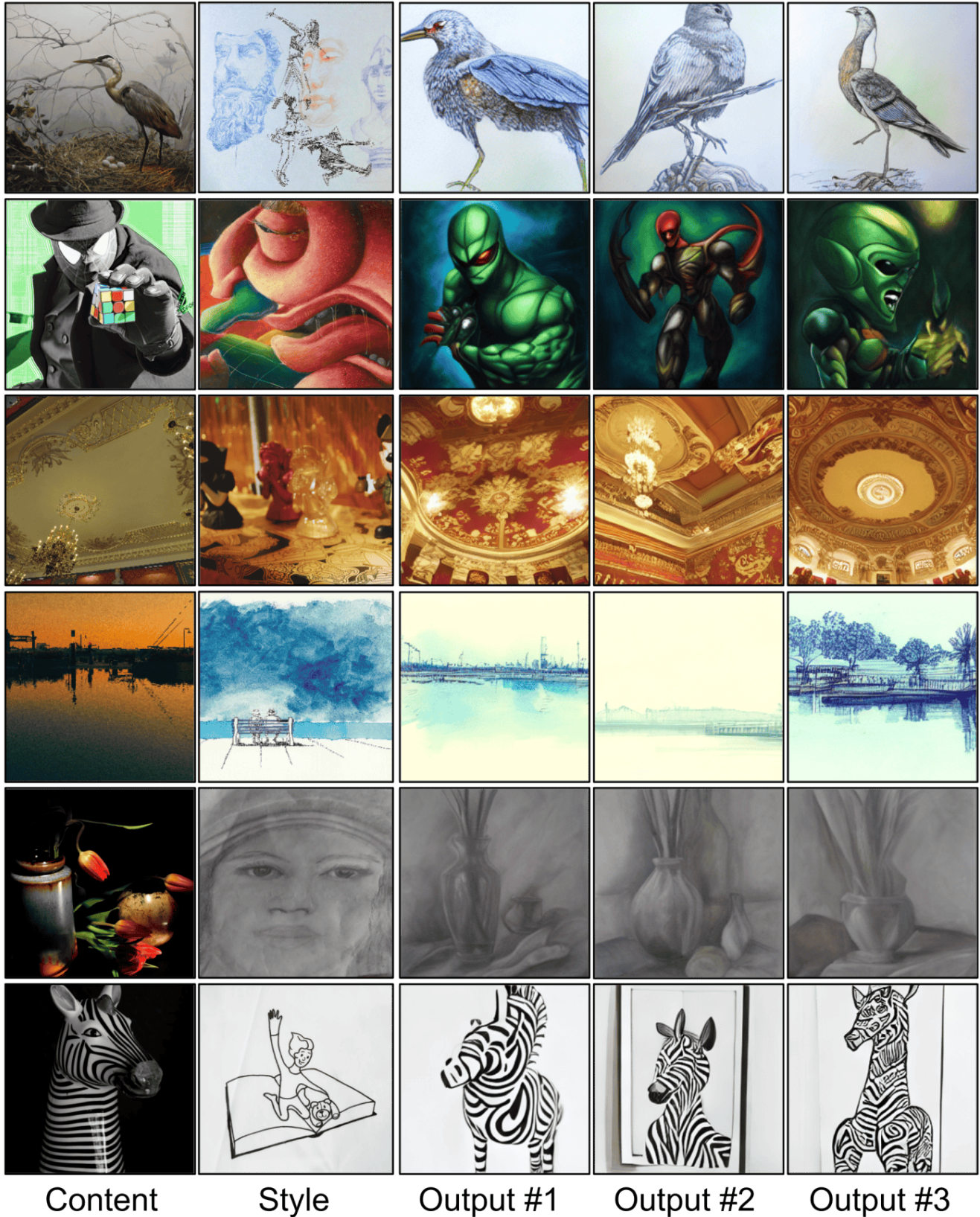


Figure 30: Diversity in fine-grained content. Images generated by PARASOL allowing flexibility in the fine-grained content details and image structure.